Electronic Supplementary Information

Nitrogen-containing andrographolide derivatives with multidrug resistance reversal effects in cancer cells

Joana Ribeiro[a], Nikoletta Szemerédi[b], Bruno M. F. Goncalves[a], Gabriella Spengler[b], Carlos A. M. Afonso[a], Maria-José U. Ferreira[a,*]

[a] Research Institute for Medicines (iMed.ULisboa), Faculty of Pharmacy, Universidade de Lisboa, Av. Prof. Gama Pinto, 1649-003 Lisbon, Portugal
[b] Department of Medical Microbiology, Albert Szent-Györgyi Health Center, Faculty of Medicine, University of Szeged, Semmelweis utca 6, 6725 Szeged, Hungary

*Corresponding Author: Maria-José Ferreira; E-mail: mjuferreira@ff.ulisboa.pt

Table of contents

1. NMR data of parental compound 1

White amorphous powder; ^{1}H-NMR (300 MHz, DMSO-d6) δ = 6.62 (1H, *td*, J = 6.8, 1.7 Hz, H-12), 5.70 (1H, *d*, J = 6.1 Hz, H-14-OH), 5.04 (1H, *d*, J = 4.9 Hz, H-3-OH), 4.91 (1H, *br t*, J = 6.1 Hz, H-14), 4.81 (1H, *br s*, H-17a), 4.63 (1H, *br s*, H-17b), 4.39 (1H, *dd*, J = 9.9, 6.1 Hz, H-15a), 4.12 (1H, *dd*, J = 7.5, 2.9 Hz, H-19-OH), 4.03 (1H, *dd*, J = 9.9, 2.1 Hz, H-15b), 3.84 (1H, *dd*, J = 11.0, 2.9 Hz, H-19a), 3.29-3.19 (2H, *m*, H-3 and H-19b), 2.46 (2H, *m*, H-11), 2.32 (2H, *m*, H-7), 1.95 (2H, *m*, H-2), 1.74 (2H, *m*, H-6), 1.63 (2H, *m*, H-1), 1.30 (1H, *m*, H-9), 1.20 (1H, *m*, H-5), 1.08 (3H, *s*, H-18), 0.66 (3H, *s*, H-20) ppm. ^{13}C-NMR (75 MHz, $CDCl_3$) δ = 169.9 (C-16), 147.6 (C-12), 146.3 (C-8), 129.0 (C-13), 108.2 (C-17), 78.4 (C-3), 74.3 (C-15), 64.5 (C-14), 62.6 (C-19), 55.5 (C-9), 54.4 (C-5), 42.3 (C-4), 38.6 (C-10), 37.5 (C-7), 36.5 (C-1), 27.9 (C-2), 23.9 (C-6 and C-11), 23.0 (C-18), 14.7 (C-20) ppm. ESI-MS (positive mode) m/z (rel. Int) 351 $[M + H]^{+}$. These data are in agreement with the literature.[1,2]

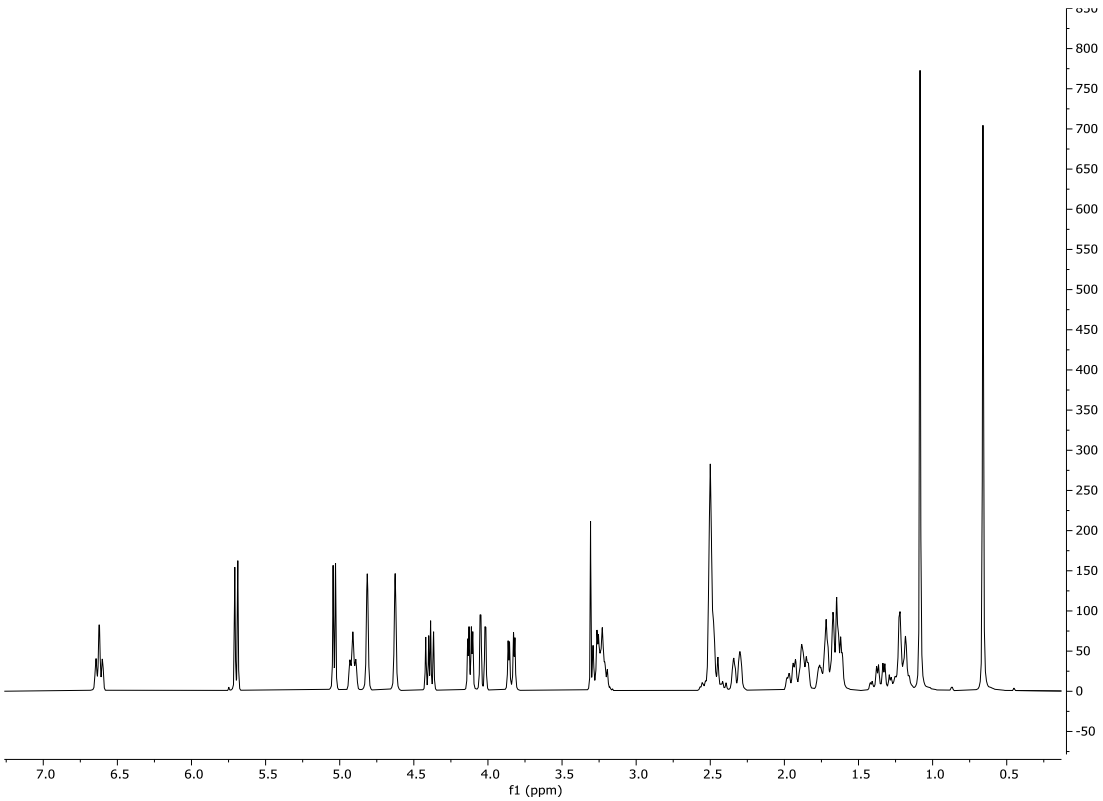

Figure S1: ^{1}H-NMR spectrum of compound **1** (300 MHz, DMSO-d6)

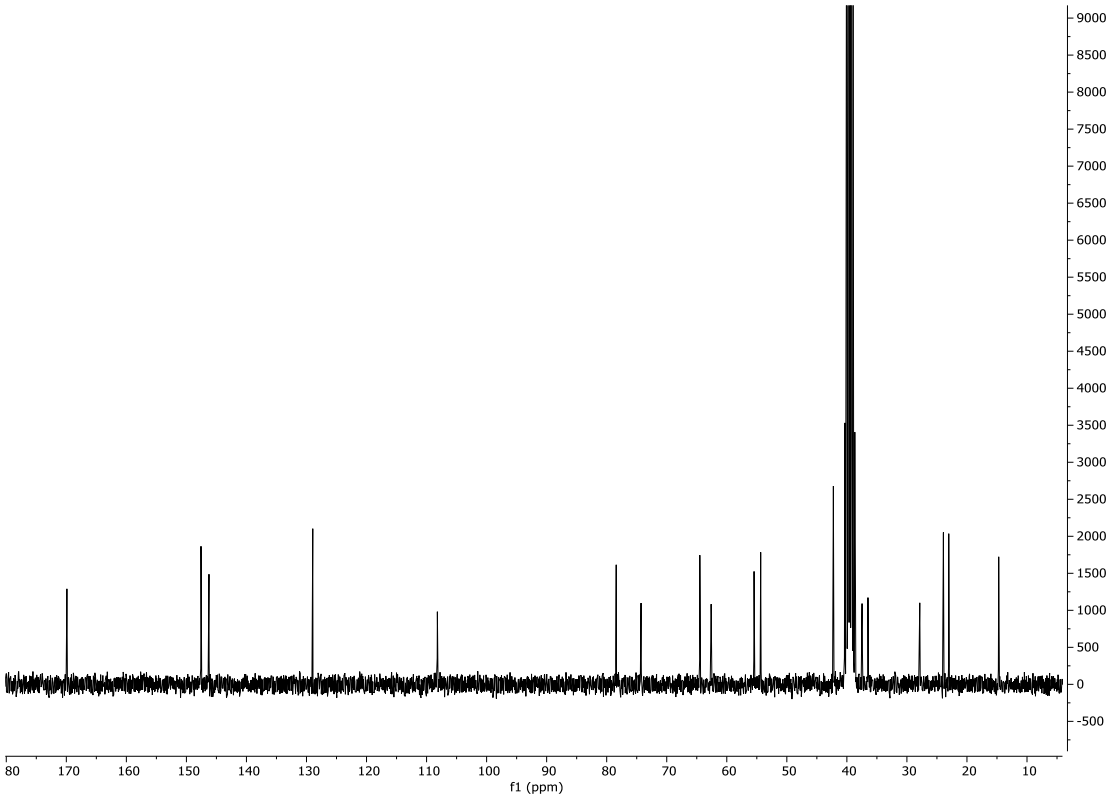

Figure S2: ^{13}C-NMR spectrum of compound **1** (75 MHz, DMSO-d6)

2. Representative 1H and 13C NMR spectra

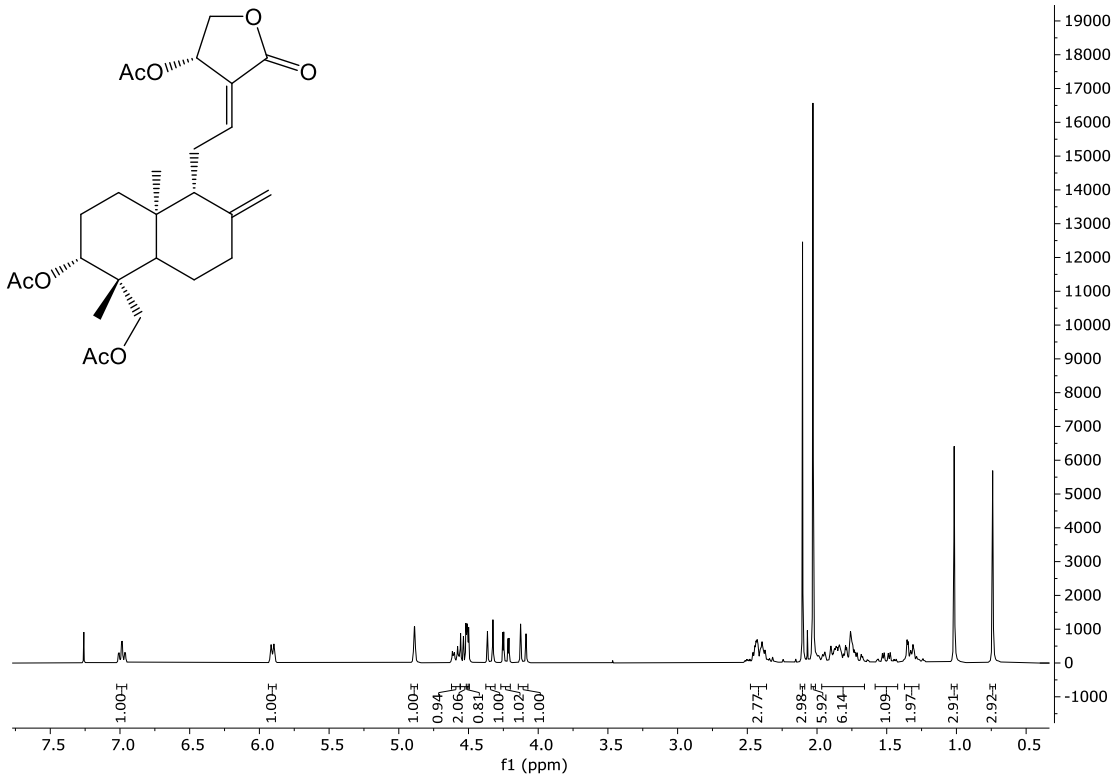

Figure S3: ^{1}H-NMR spectrum of compound **2** (300 MHz, $CDCl_3$)

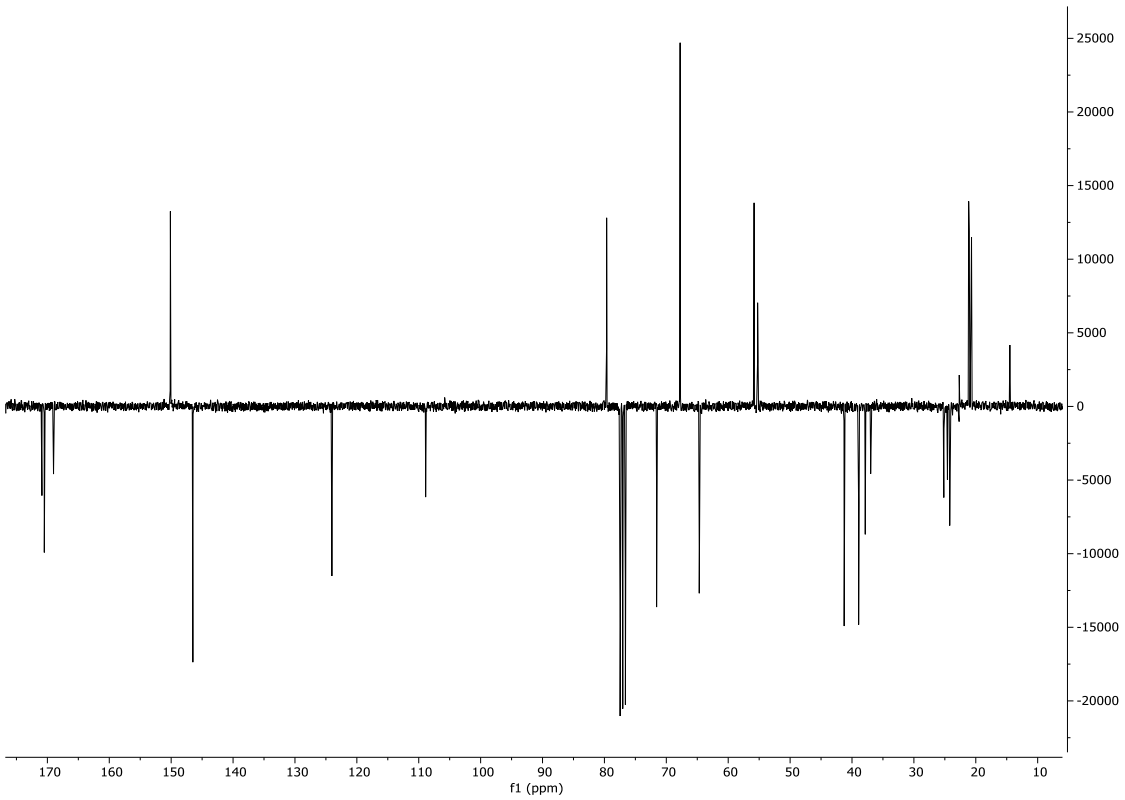

Figure S4: ^{13}C-APT NMR spectrum of compound **2** (75 MHz, $CDCl_3$)

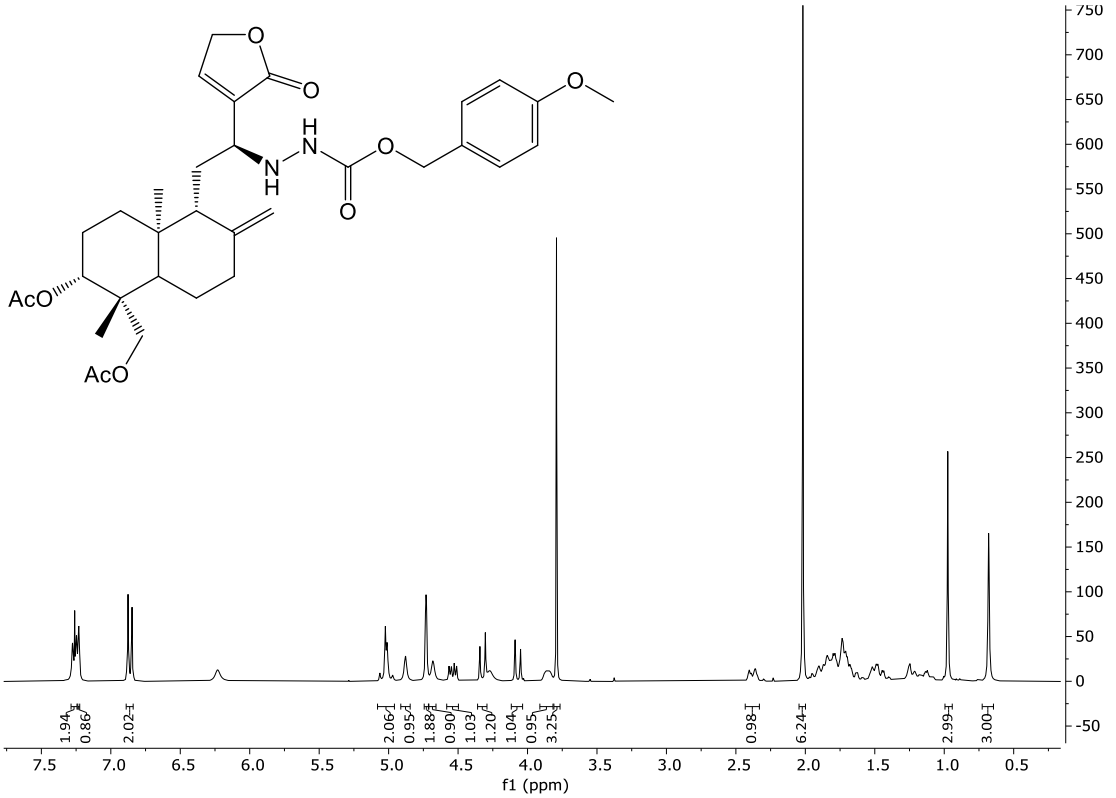

Figure S5: ^{1}H-NMR spectrum of compound **4** (300 MHz, $CDCl_3$)

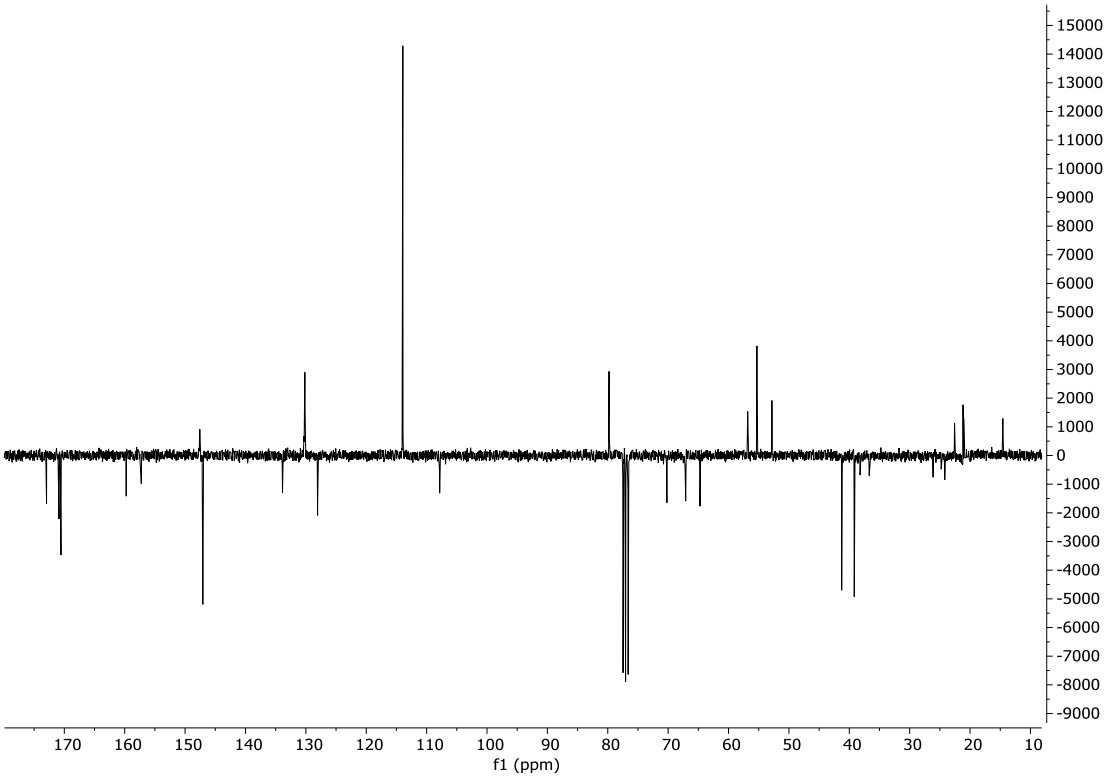

Figure S6: ^{13}C-APT NMR spectrum of compound **4** (75 MHz, $CDCl_3$)

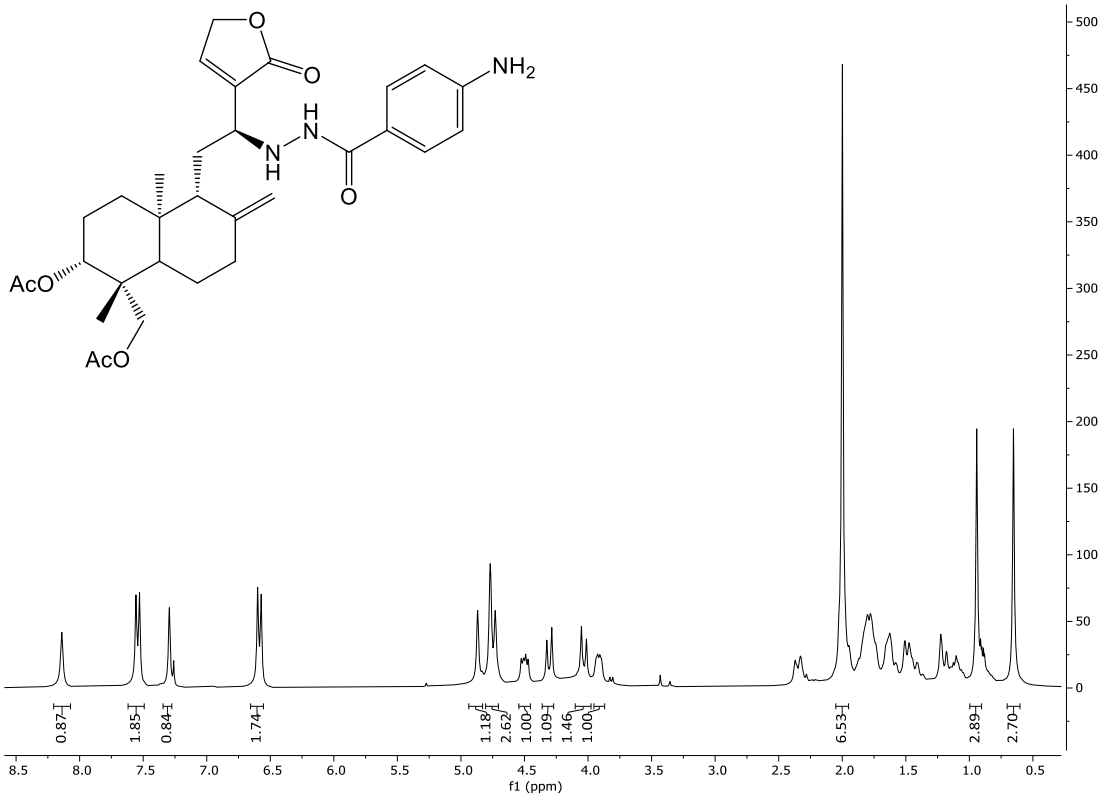

Figure S7: ^{1}H-NMR spectrum of compound **5** (300 MHz, $CDCl_3$)

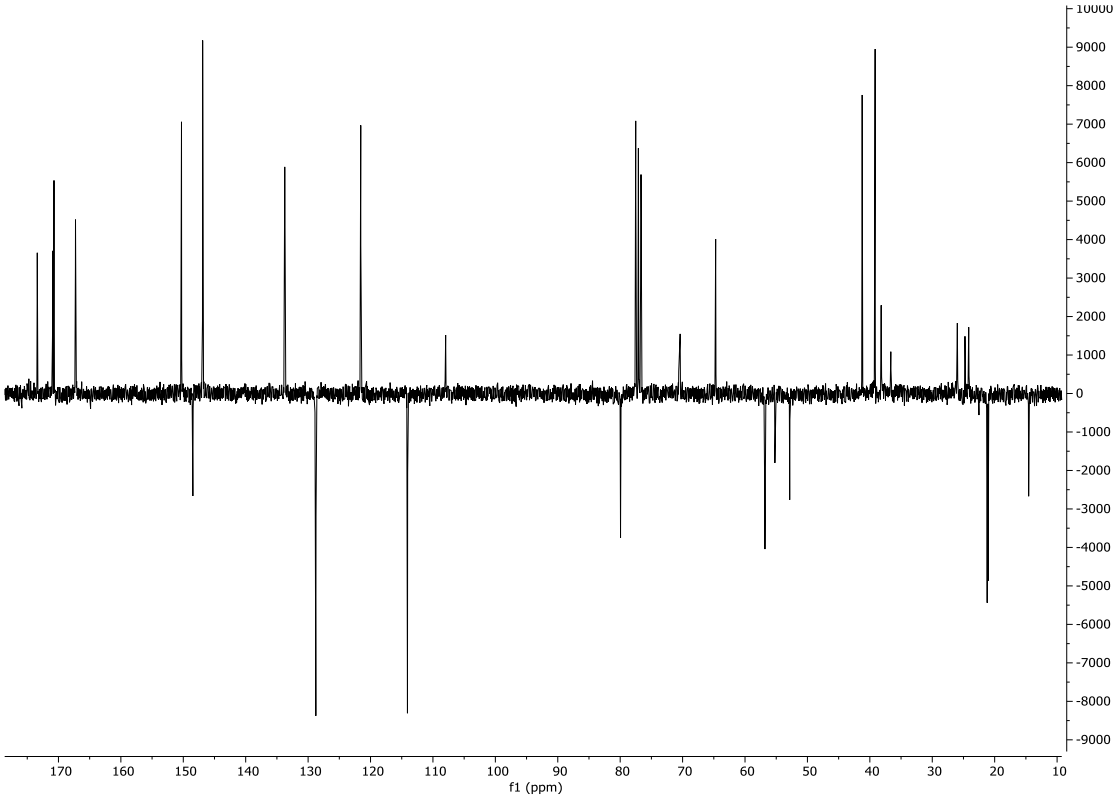

Figure S8: ^{13}C-APT NMR spectrum of compound **5** (75 MHz, $CDCl_3$)

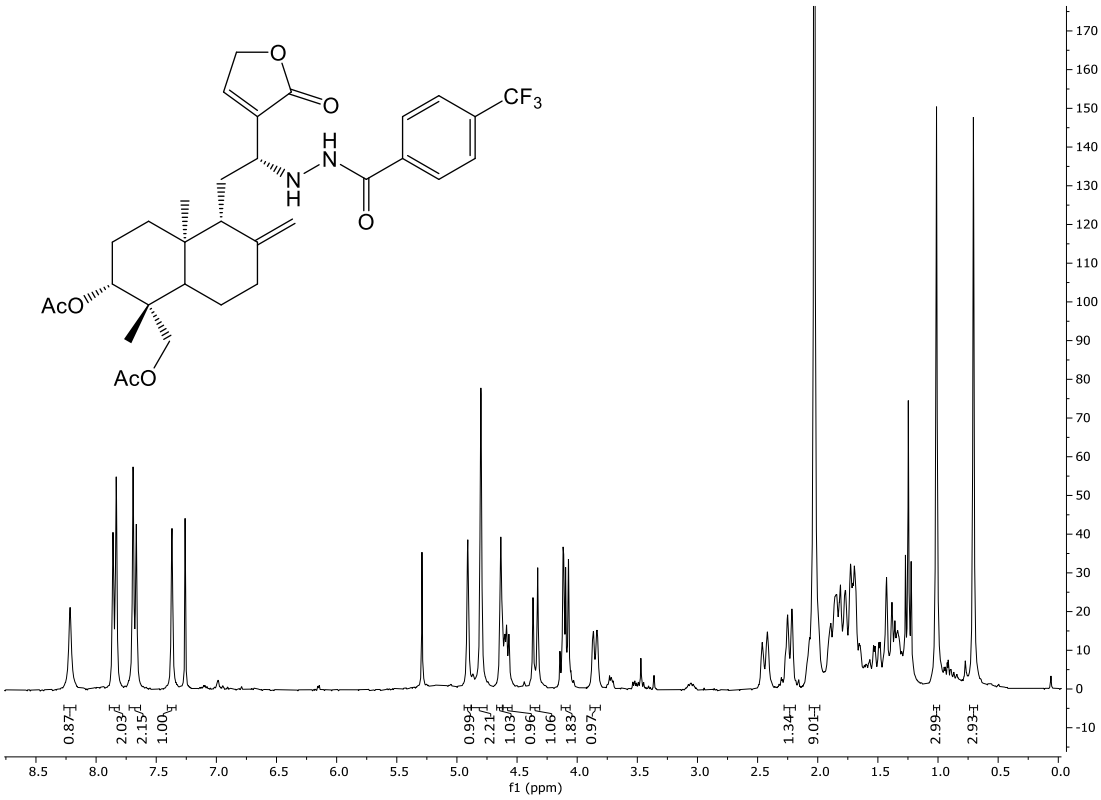

Figure S9: ^{1}H-NMR spectrum of compound **7** (300 MHz, $CDCl_3$)

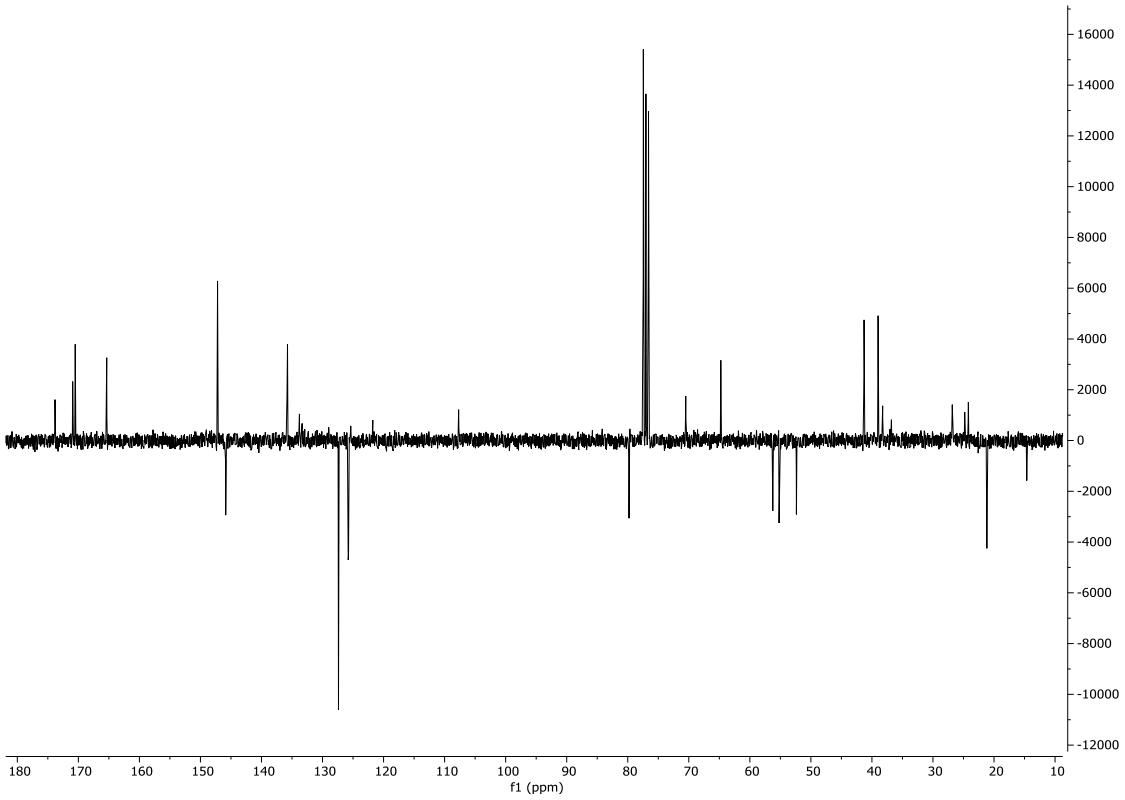

Figure S10: ^{13}C-APT NMR spectrum of compound **7** (75 MHz, $CDCl_3$)

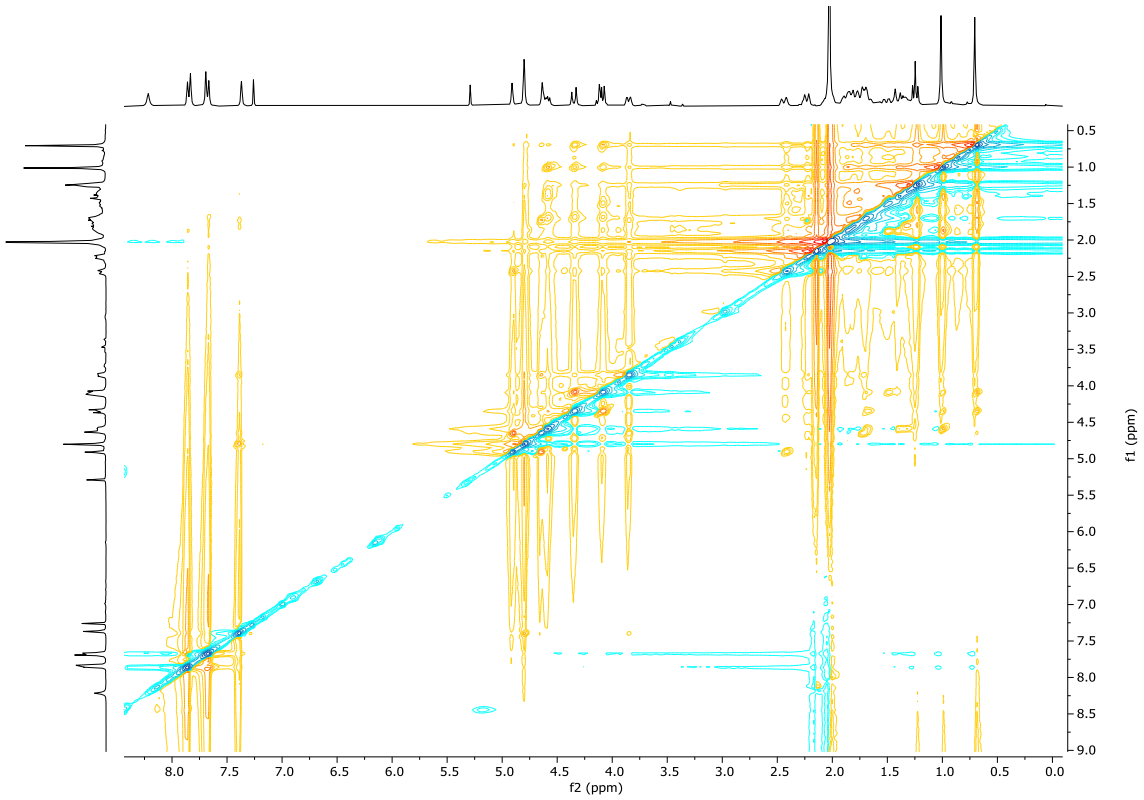

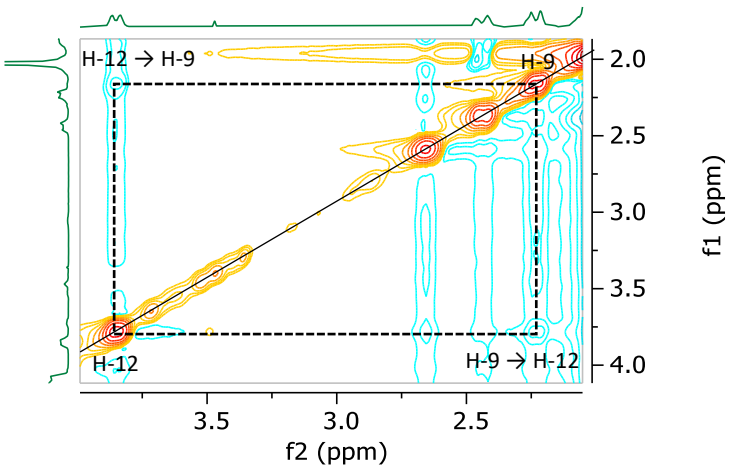

Figure S11: NOESY spectrum and expansion of compound **7** (300 MHz, $CDCl_3$)

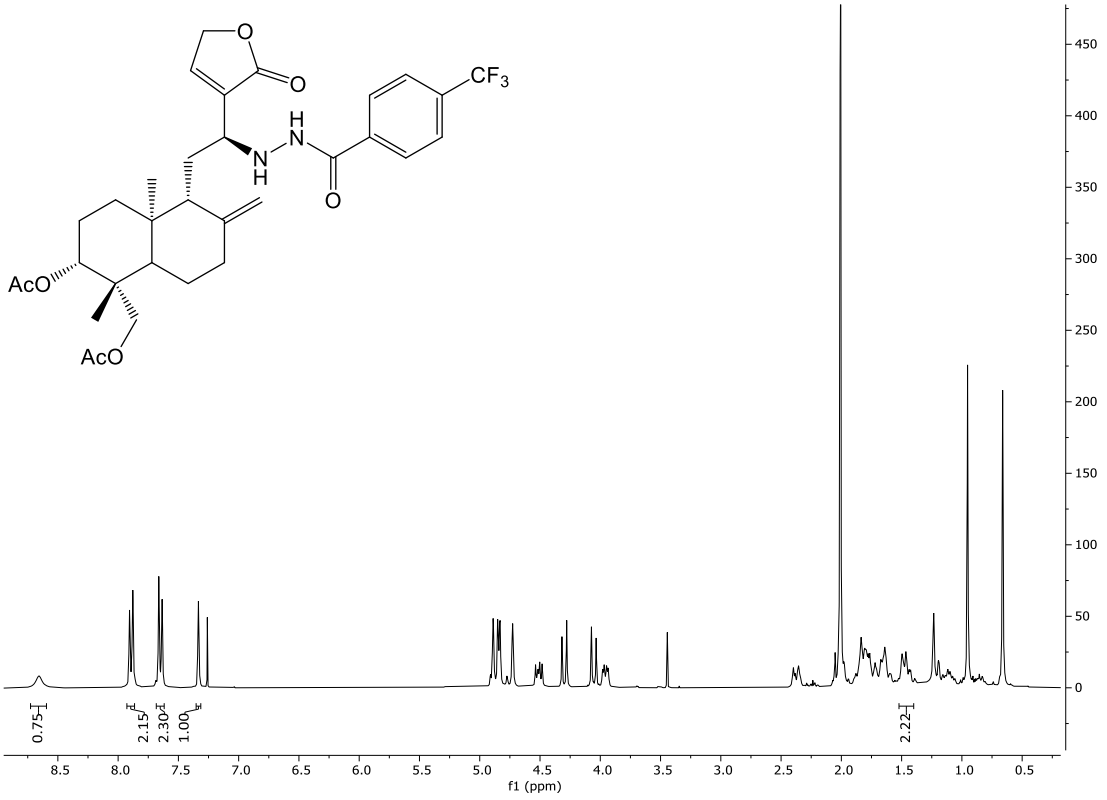

Figure S12: ^{1}H-NMR spectrum of compound **8** (300 MHz, $CDCl_3$)

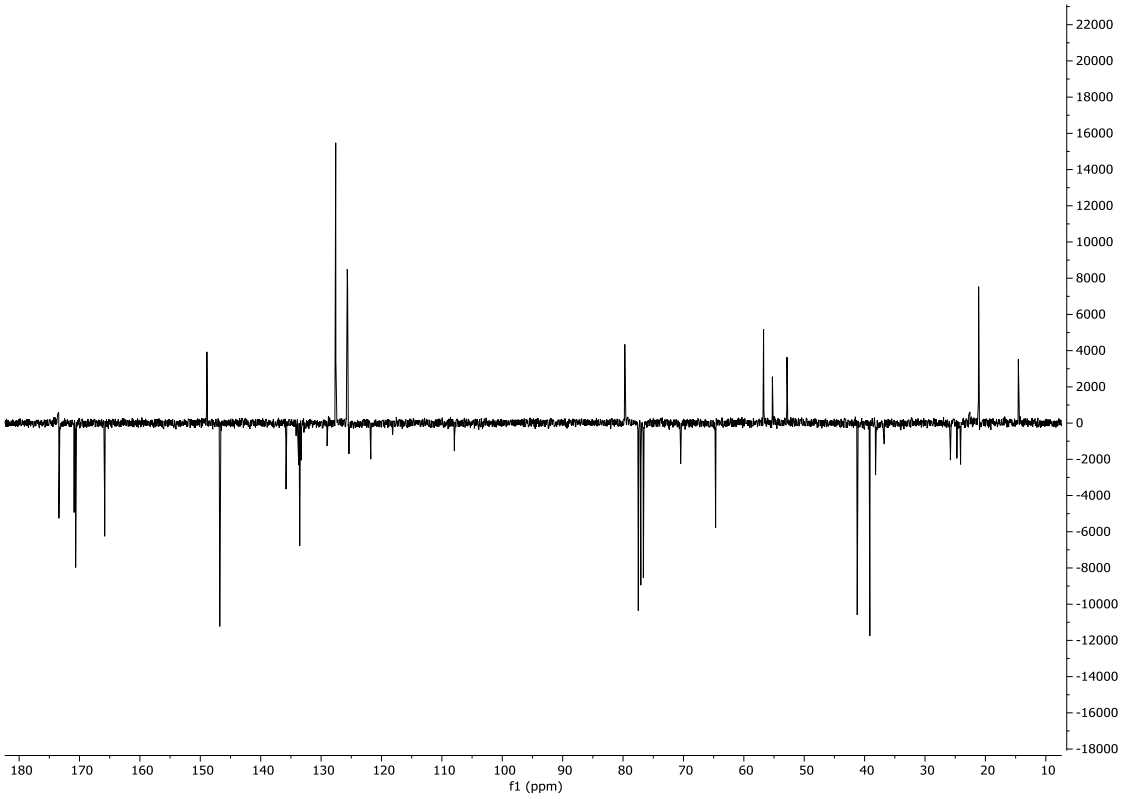

Figure S13: ^{13}C-APT NMR spectrum of compound **8** (75 MHz, $CDCl_3$)

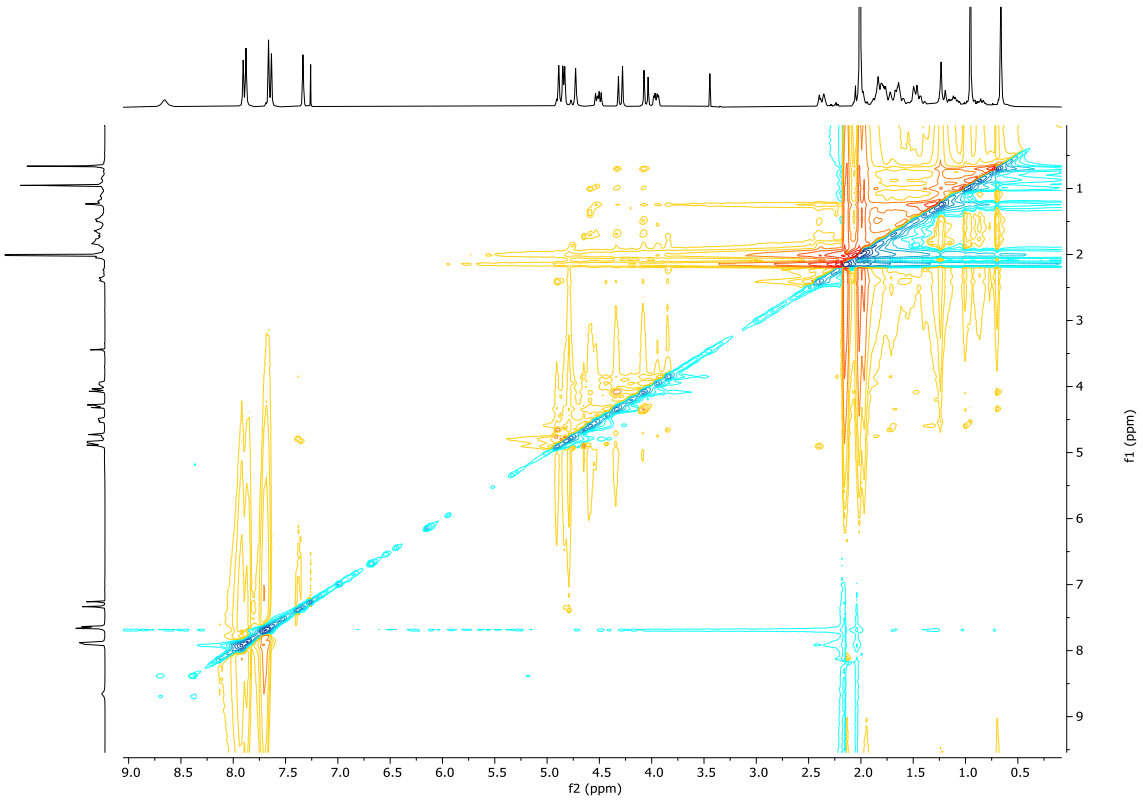

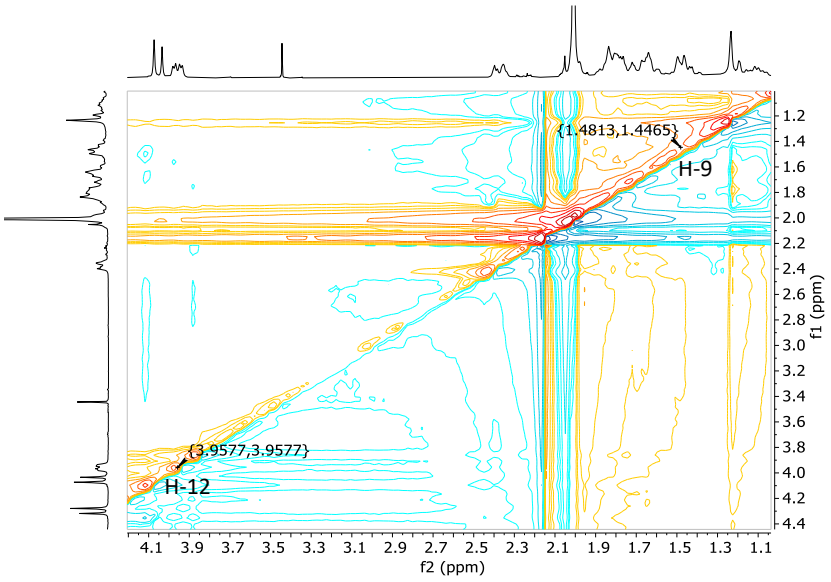

Figure S14: NOESY spectrum and expansion of compound **8** (500 MHz, $CDCl_3$)

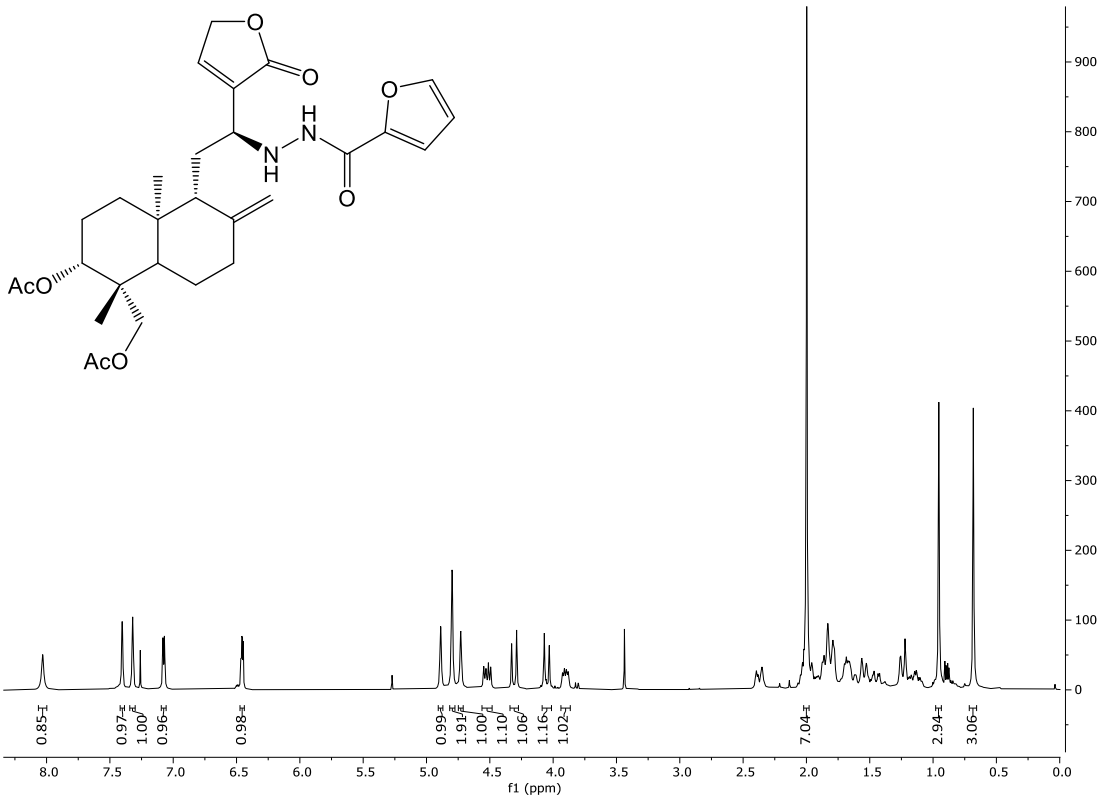

Figure S15: ^{1}H-NMR spectrum of compound **10** (300 MHz, $CDCl_3$)

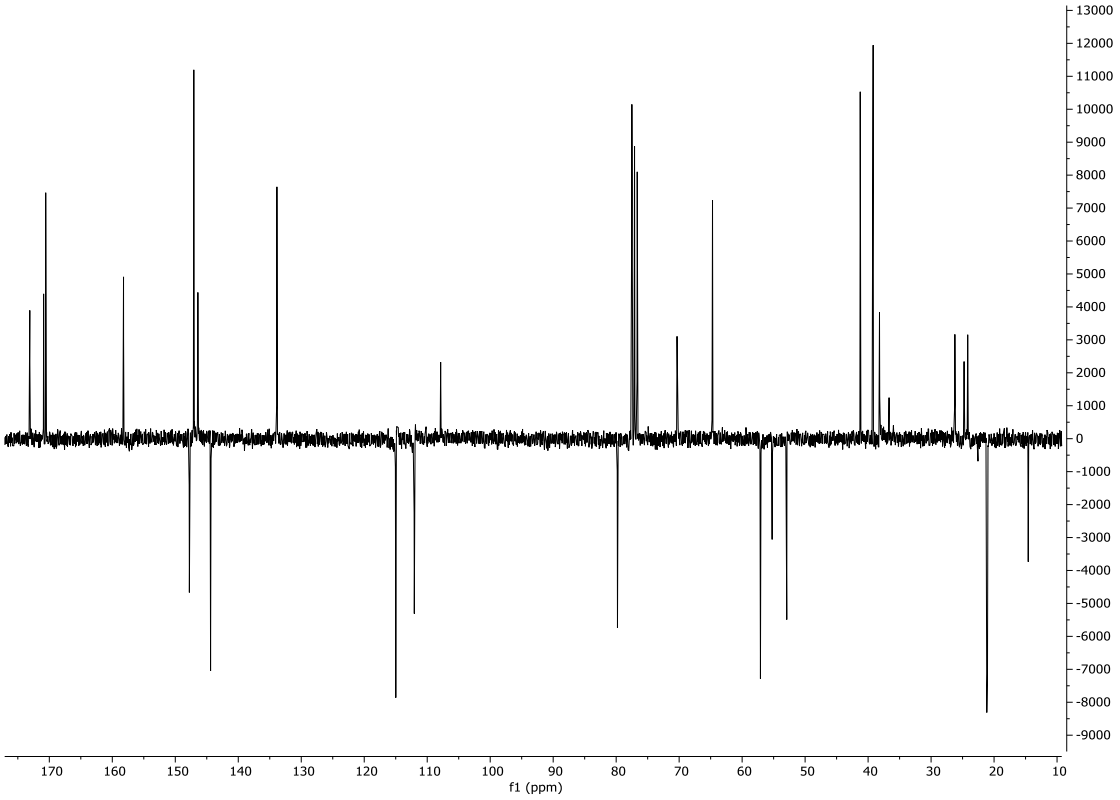

Figure S16: ^{13}C-APT NMR spectrum of compound **10** (75 MHz, $CDCl_3$)

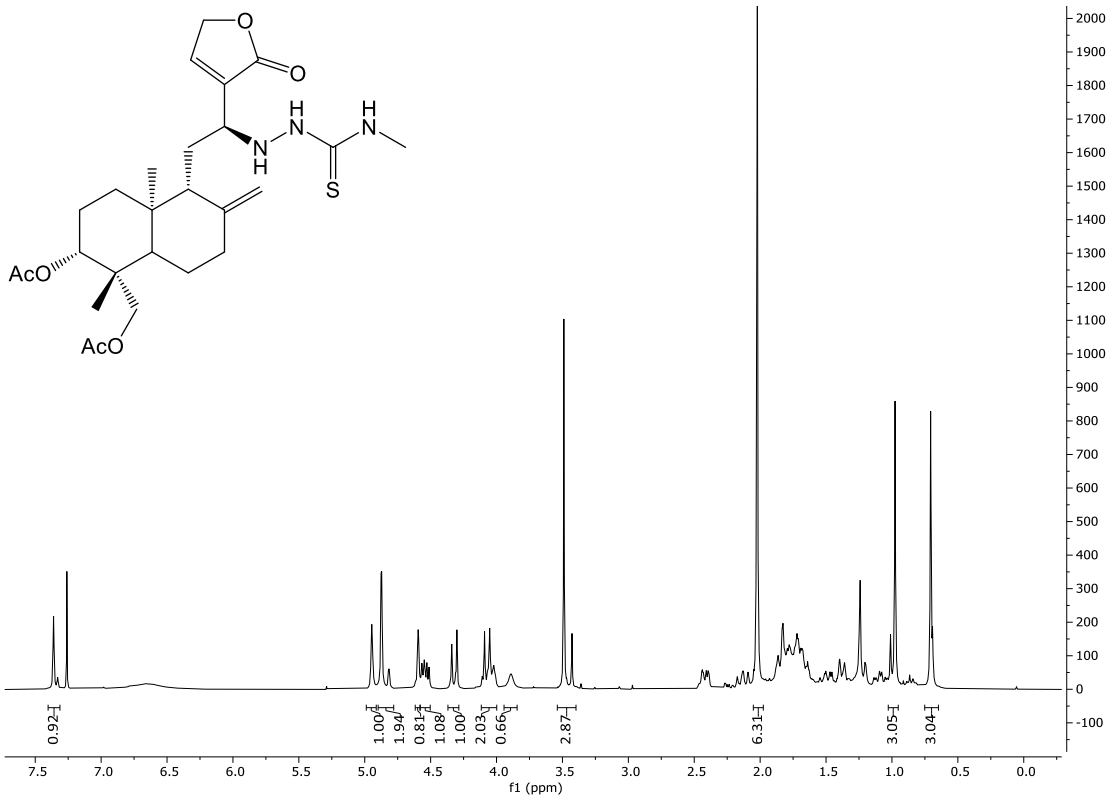

Figure S17: ^{1}H-NMR spectrum of compound **12** (300 MHz, $CDCl_3$)

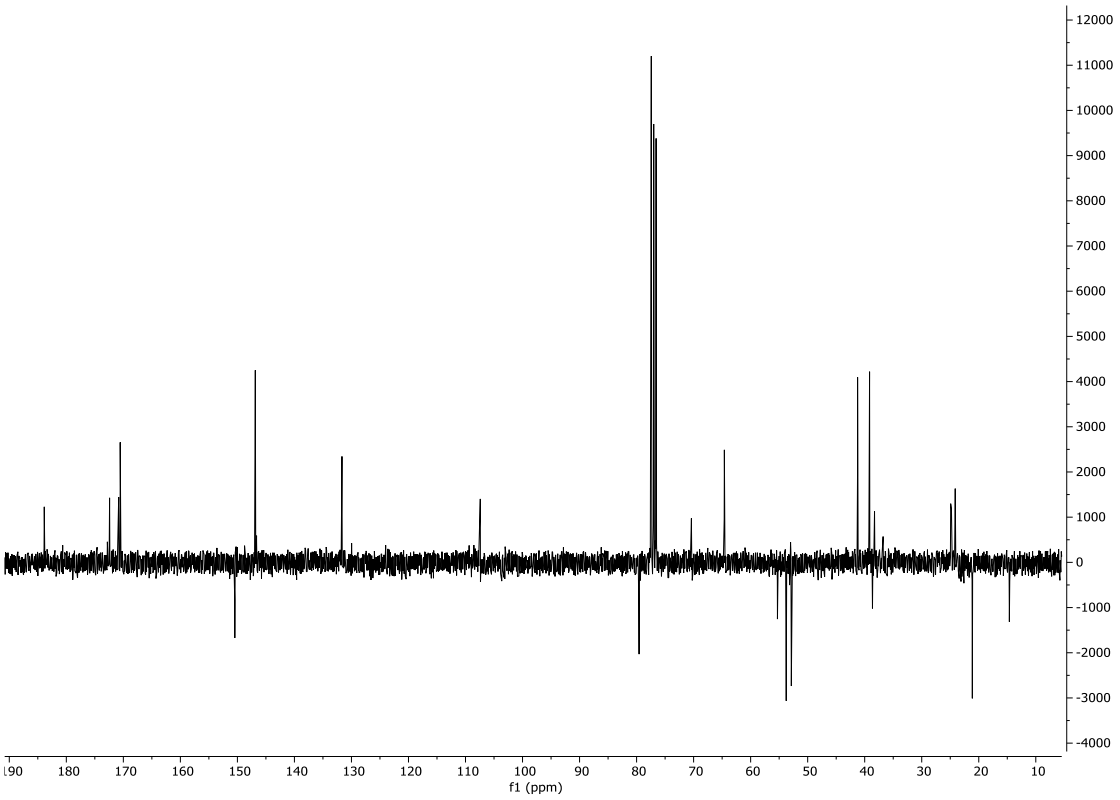

Figure S18: ^{13}C-APT NMR spectrum of compound **12** (75 MHz, $CDCl_3$)

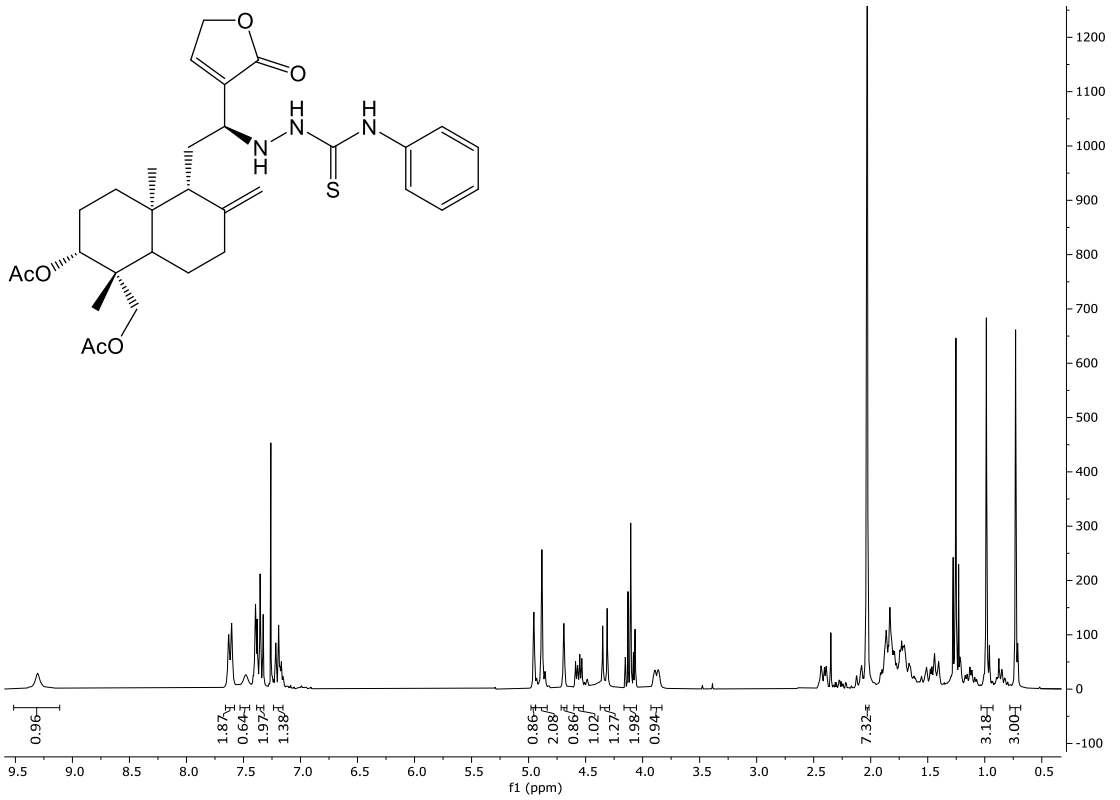

Figure S19: ^{1}H-NMR spectrum of compound **17** (300 MHz, $CDCl_3$)

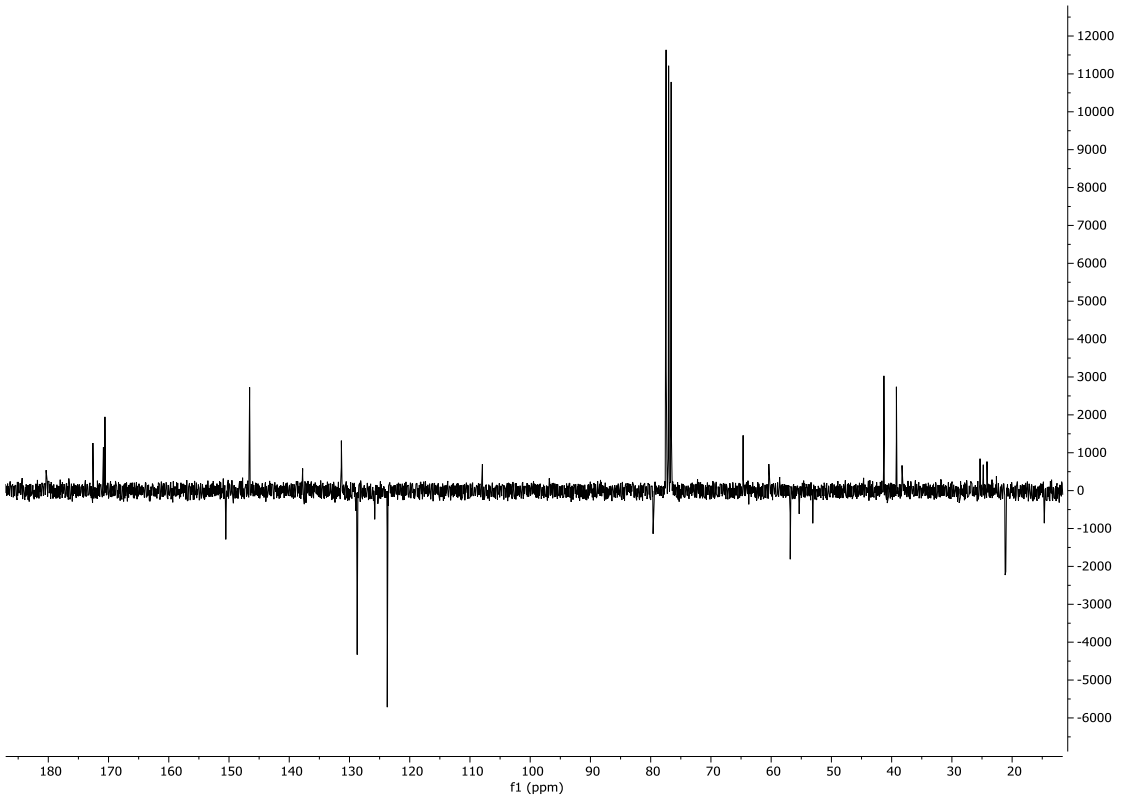

Figure S20: ^{13}C-APT NMR spectrum of compound **17** (75 MHz, $CDCl_3$)

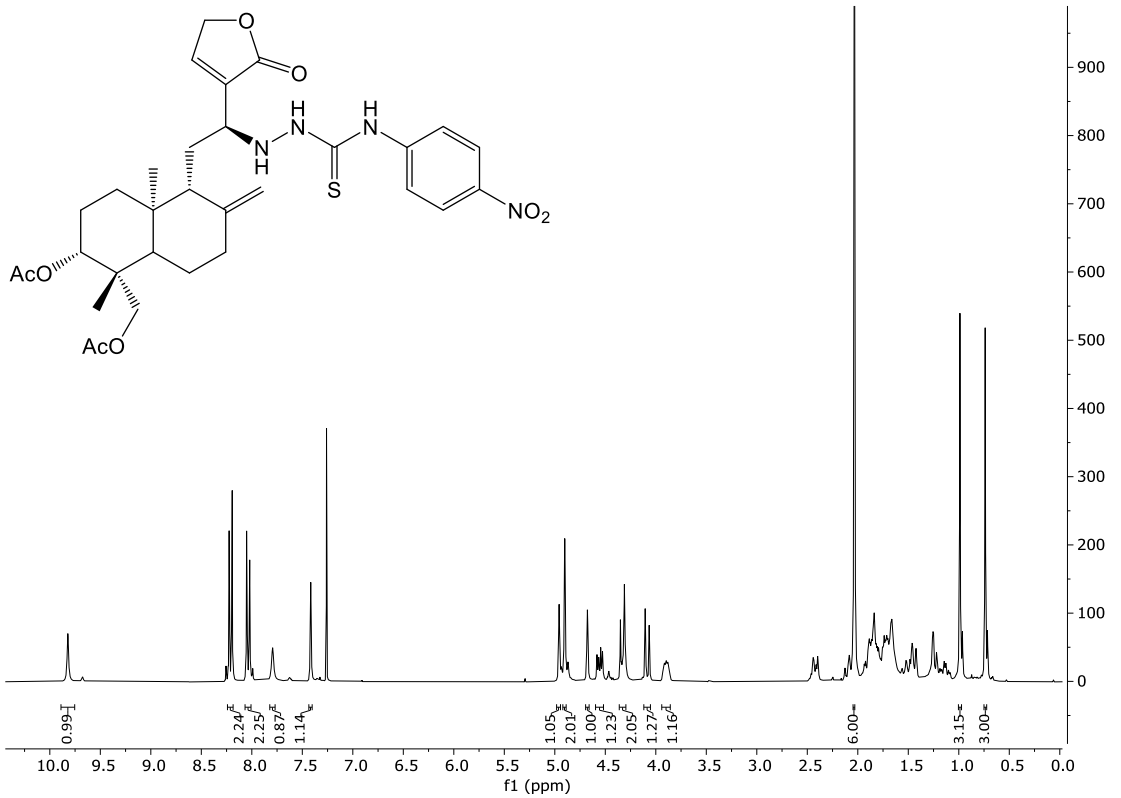

Figure S21: ^{1}H-NMR spectrum of compound **21** (300 MHz, $CDCl_3$)

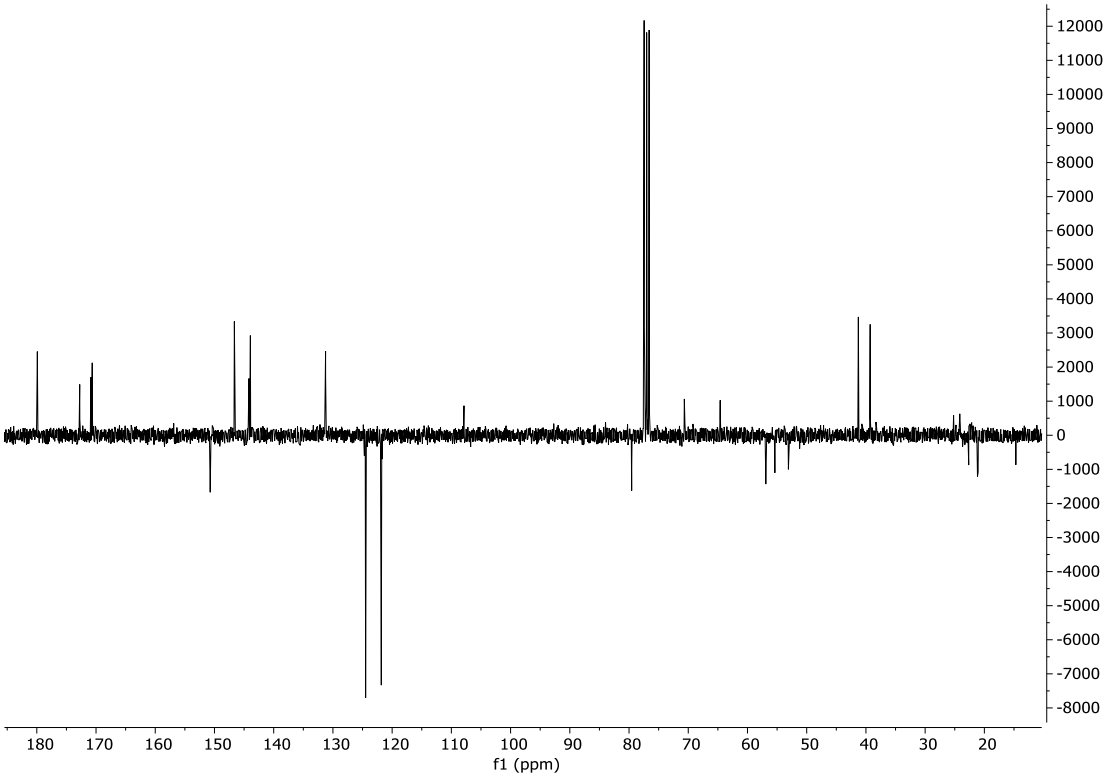

Figure S22: ^{13}C-APT NMR spectrum of compound **21** (75 MHz, $CDCl_3$)

3. Rhodamine-123 accumulation assay (compounds 1-25)

Table S1: P-pg inhibitory activity of compounds 1 – 25 on MDR-transfected mouse T-lymphoma cells.

Compound	R	Conc. (µM)	FAR[a]	FSC[b]	SSC[c]	FL-1[d]
PAR	-	-	-	2362	941	76.70
MDR	-	-	-	2444	1063	2.13
1	Andrographolide	2	0.96	2343	1326	1.32
		20	0.82	2242	1355	1.12
2	Triacetyl Andrographolide	2	1.95	1979	1395	2.68
		20	38.65	2367	1279	53.10
3	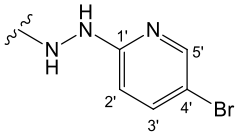	0.2	2.34	2461	1124	16.00
		2	16.12	2413	1162	110.00
4	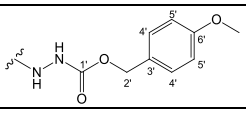	2	1.21	2307	1037	1.66
		20	64.99	2307	1037	68.10
5	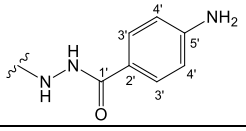	0.2	0.48	2501	1131	3.30
		2	0.48	2432	1116	3.28
6	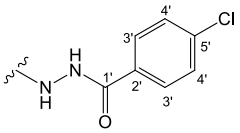	0.2	1.56	2469	1131	10.60
		2	3.36	2431	1144	22.90
7	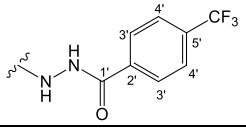	0.2	1.63	2469	1129	11.10
		2	5.19	2433	1148	35.40
8	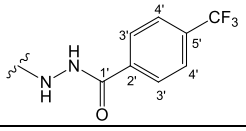	0.2	0.37	2463	1126	2.54
		2	2.27	2413	1210	15.50
9	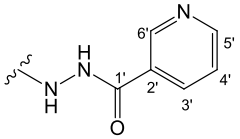	0.2	0.49	2472	1124	3.36
		2	0.32	2426	1191	2.21
10	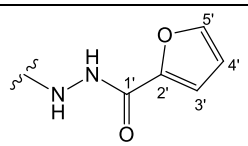	0.2	2.32	2503	1092	15.80
		2	4.28	2506	1248	29.20
11		0.2	0.54	2500	1106	3.67

	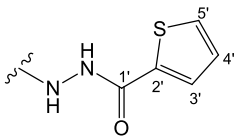	2	1.89	2448	1179	12.90

Table S1: Continuation

Compound	R	Conc. (µM)	FAR[a]	FSC[b]	SSC[c]	FL-1[d]
12	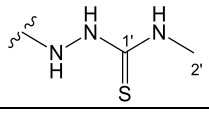	2	0.88	2299	1013	1.21
		20	41.85	2271	1012	57.50
13	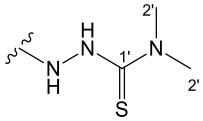	2	58.18	2142	1275	112.00
		20	61.30	2092	1296	118.00
14	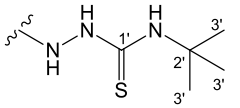	2	1.20	2289	1002	1.65
		20	43.52	2192	984	59.80
15	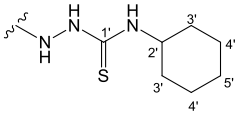	2	18.13	2225	1138	34.90
		20	64.94	2155	1217	125.0
16	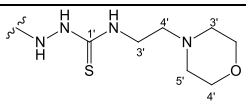	2	1.37	2216	1128	2.63
		20	50.23	2177	1163	96.70
17	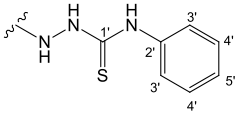	2	7.90	2226	1202	15.20
		20	55.07	2154	1144	106.00
18	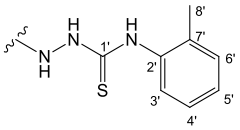	2	1.06	2302	1026	1.46
		20	37.12	2247	1037	51.50
19	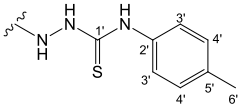	2	18.86	2154	1264	36.30
		20	60.26	2067	1357	116.00
20	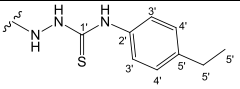	2	61.30	2160	1271	118.00
		20	79.48	2107	1300	153.00
21	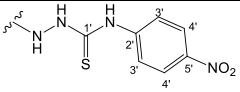	2	27.27	2226	1167	52.50
		20	51.95	2261	400	100.00
22	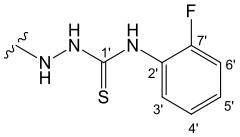	2	1.03	2319	1000	1.41
		20	79.33	2255	1060	109.00
23	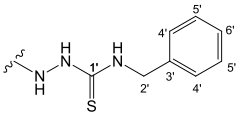	2	1.71	2260	1120	3.30
		20	57.14	2199	1200	110.0
24		2	14.29	2449	493	27.50

	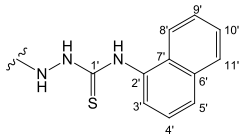	20	33.46	2090	576	64.40

Table S1: Continuation

Compound	R	Conc. (µM)	FAR[a]	FSC[b]	SSC[c]	FL-1[d]
25	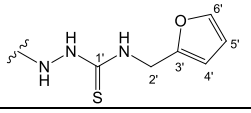	2	1.27	2164	1397	2.44
		20	31.12	2099	1300	59.90
Verapamil	-	20	5.14	2349	1222	9.90
DMSO	-	2%	0.96	2113	1230	1.85

[a]FAR (fluorescence activity ratio) values were determined by using the equation shown in section 4.5. Verapamil at 2 and 20 µM was used as positive control. DMSO 2% was used as negative control;
[b]FSC: Forward scatter count of cells in the sample; [c]SSC: Side scatter count of cells in the sample;
[d]FL-1: Mean fluorescence intensity of the cells.

4. Flow cytometry data

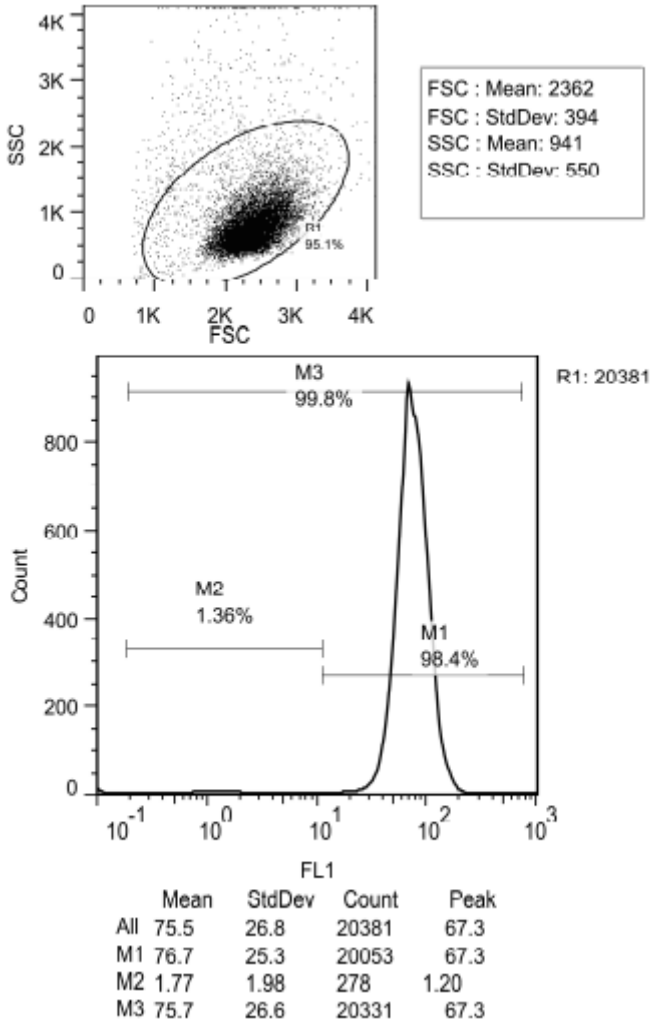

Figure S23: Flow cytometry data for sensitive L5178Y mouse T-lymphoma cells (PAR)

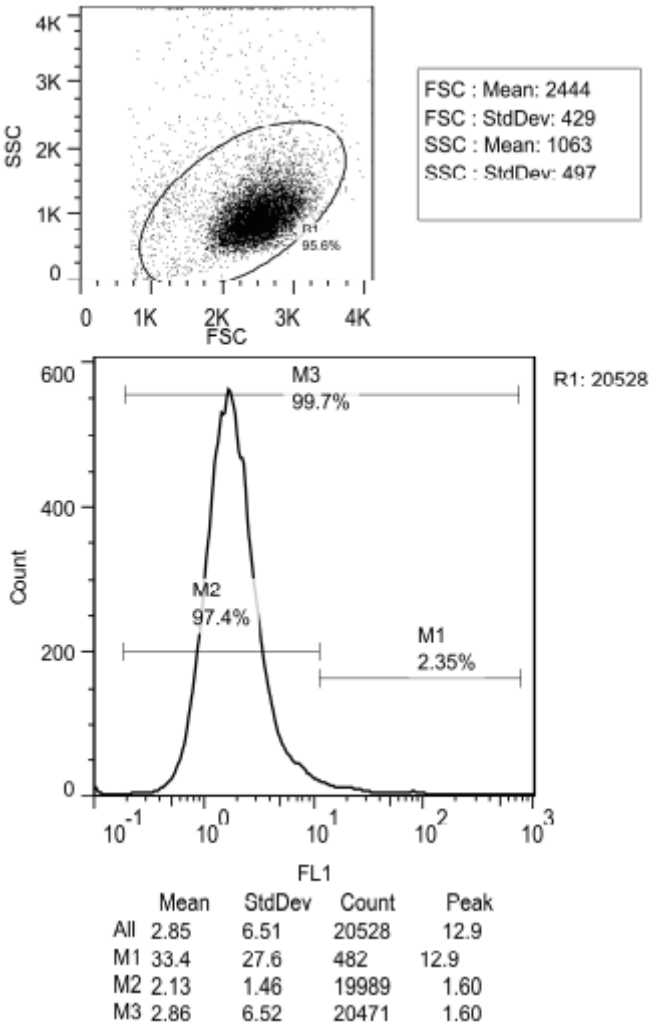

Figure S24: Flow cytometry data for resistant human *ABCB1*-gene transfected L5178Y subline (MDR)

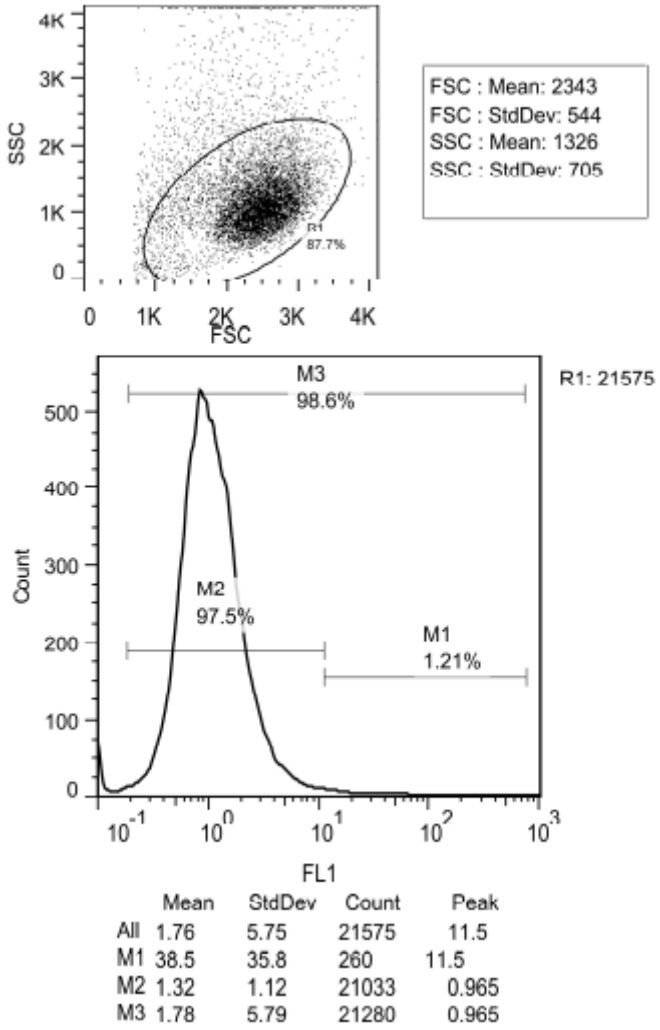

Figure S25: Flow cytometry data for compound **1** tested at 2 µM in resistant human *ABCB1*-gene transfected L5178Y subline (MDR)

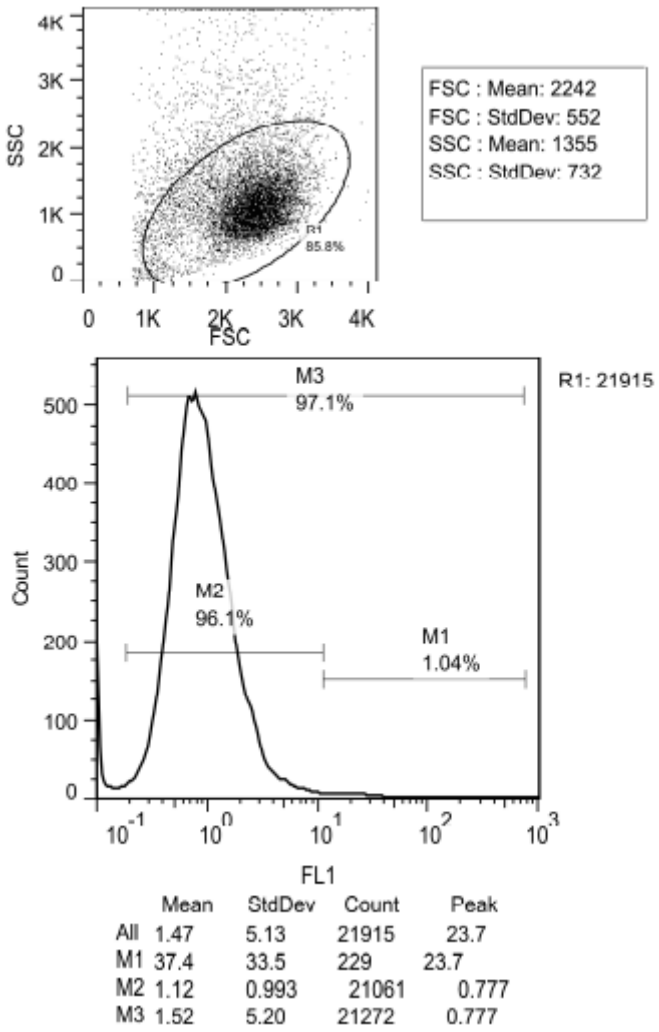

Figure S26: Flow cytometry data for compound **1** tested at 20 µM in resistant human *ABCB1*-gene transfected L5178Y subline (MDR)

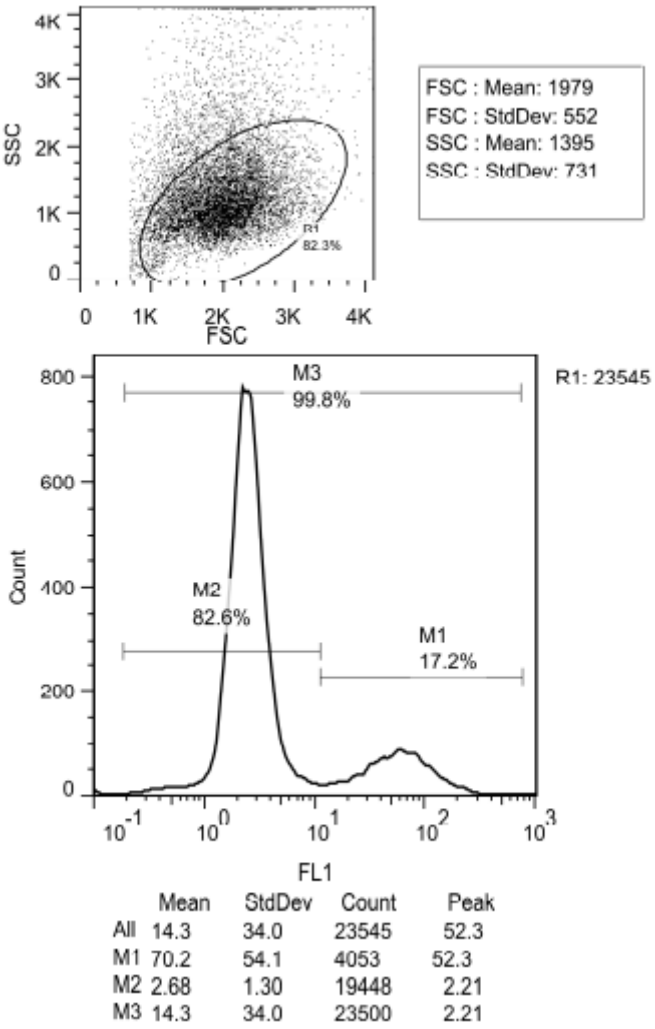

Figure S27: Flow cytometry data for compound **2** tested at 2 µM in resistant human *ABCB1*-gene transfected L5178Y subline (MDR)

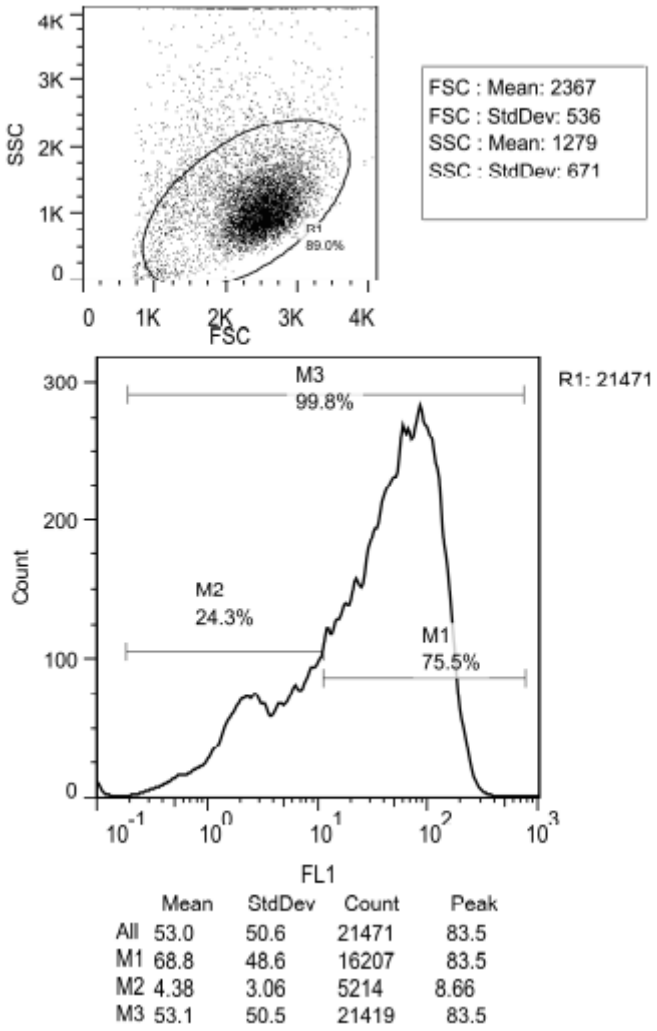

Figure S28: Flow cytometry data for compound **2** tested at 20 µM in resistant human *ABCB1*-gene transfected L5178Y subline (MDR)

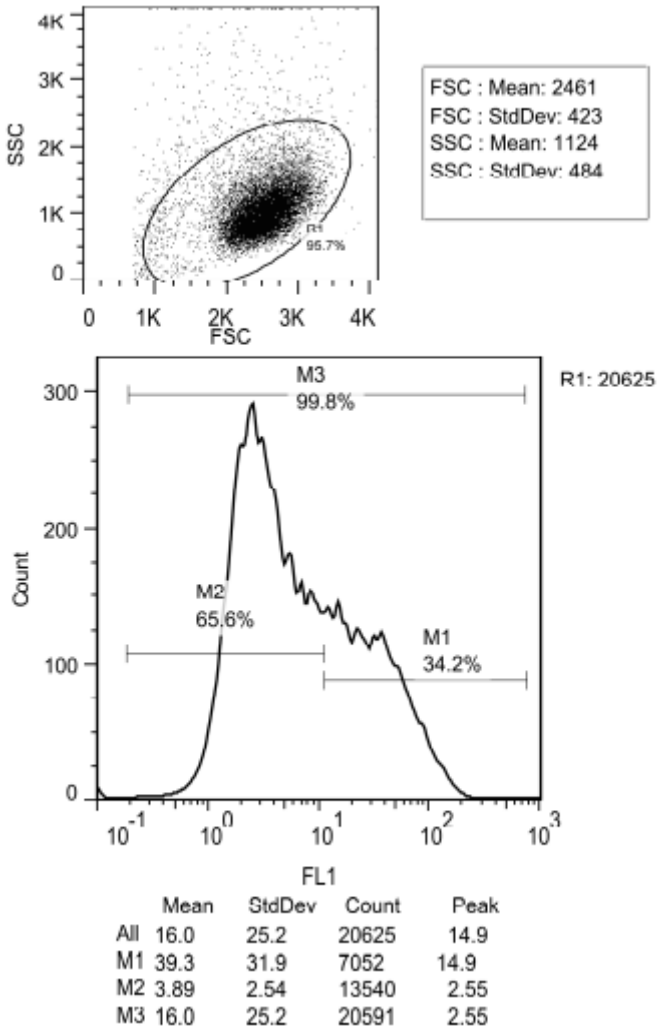

Figure S29: Flow cytometry data for compound **3** tested at 0.2 µM in resistant human *ABCB1*-gene transfected L5178Y subline (MDR)

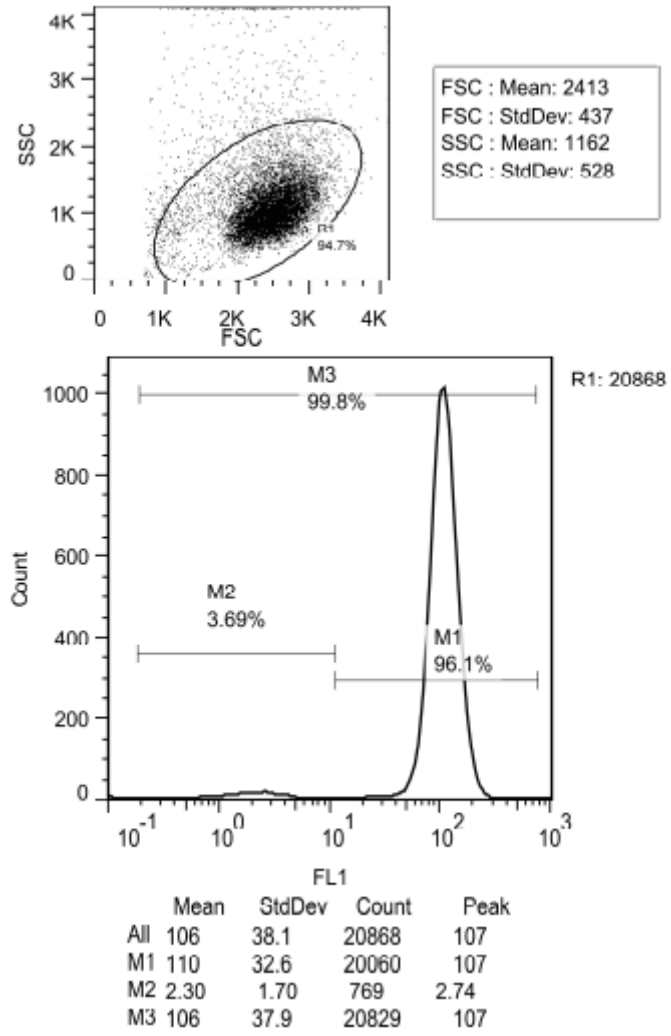

Figure S30: Flow cytometry data for compound **3** tested at 2 µM in resistant human *ABCB1*-gene transfected L5178Y subline (MDR)

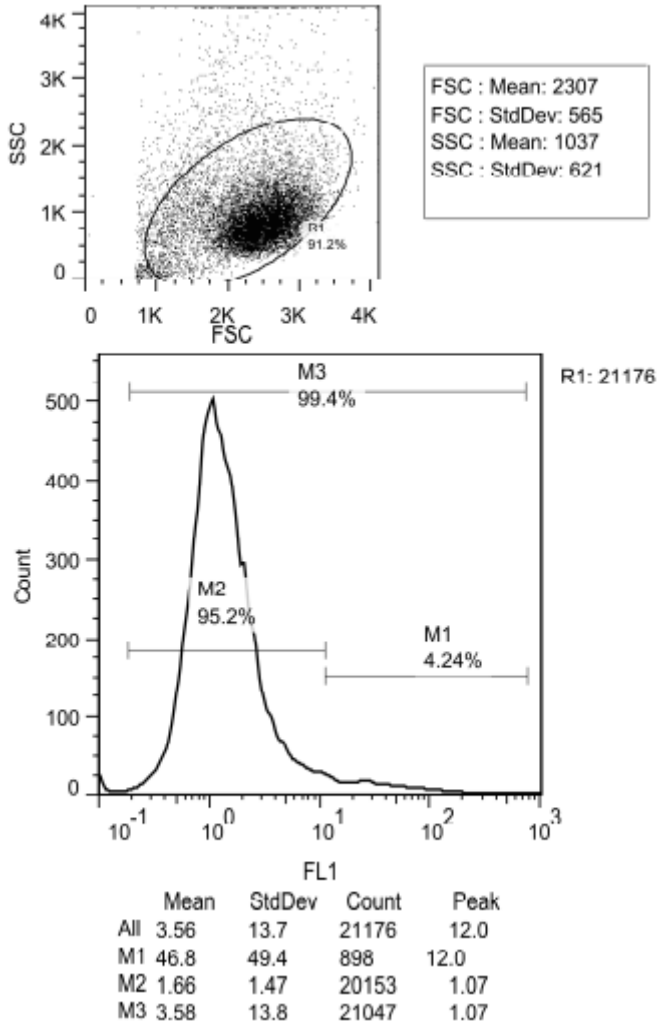

Figure S31: Flow cytometry data for compound **4** tested at 2 µM in resistant human *ABCB1*-gene transfected L5178Y subline (MDR)

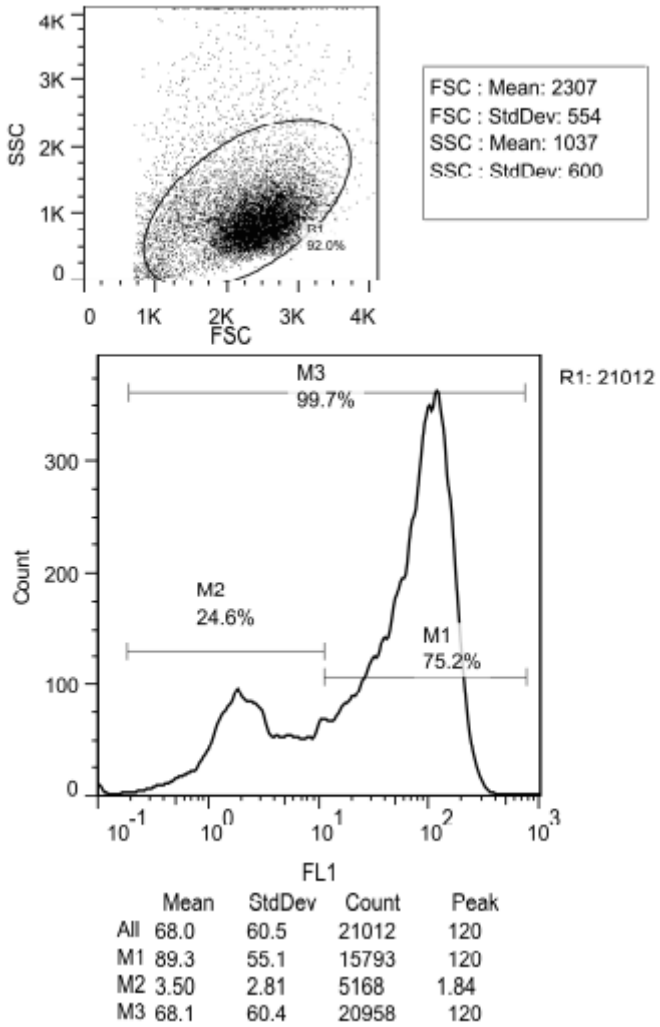

Figure S32: Flow cytometry data for compound **4** tested at 20 µM in resistant human *ABCB1*-gene transfected L5178Y subline (MDR)

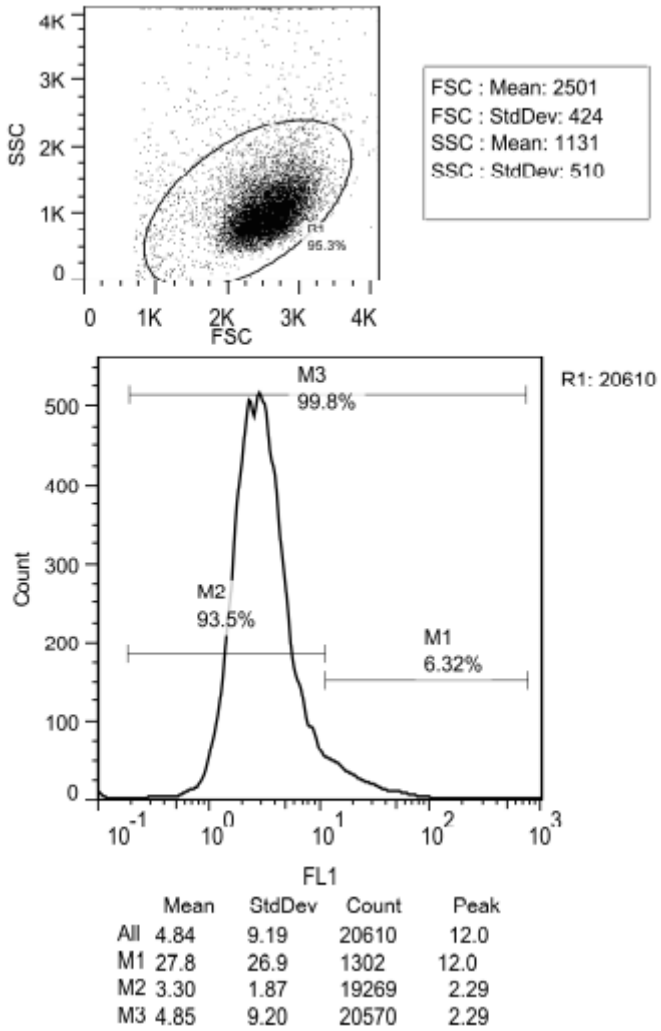

Figure S33: Flow cytometry data for compound **5** tested at 0.2 µM in resistant human *ABCB1*-gene transfected L5178Y subline (MDR)

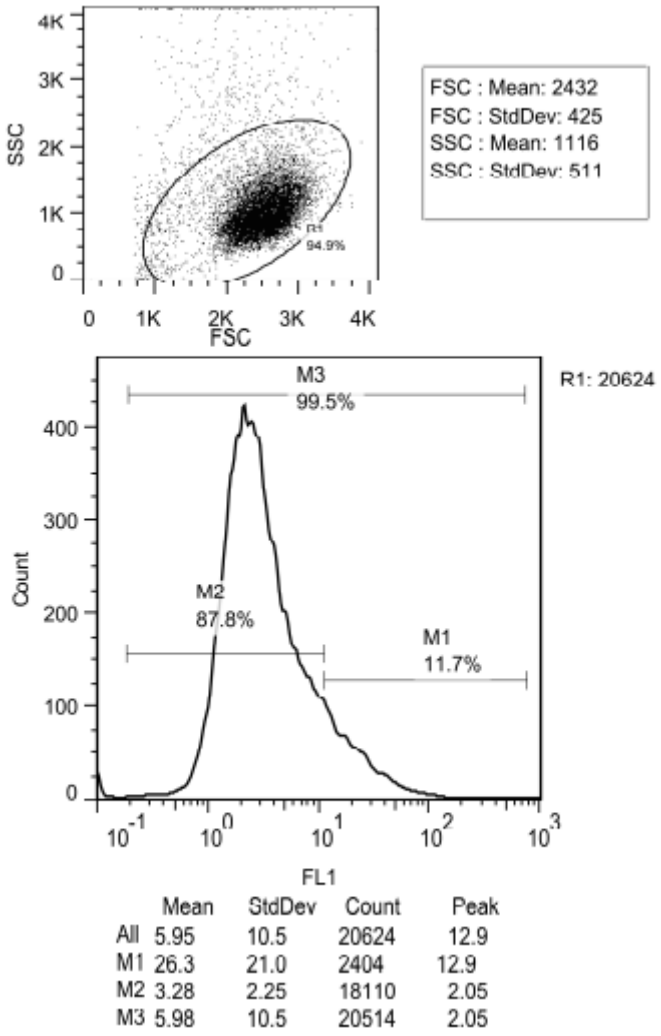

Figure S34: Flow cytometry data for compound **5** tested at 2 µM in resistant human *ABCB1*-gene transfected L5178Y subline (MDR)

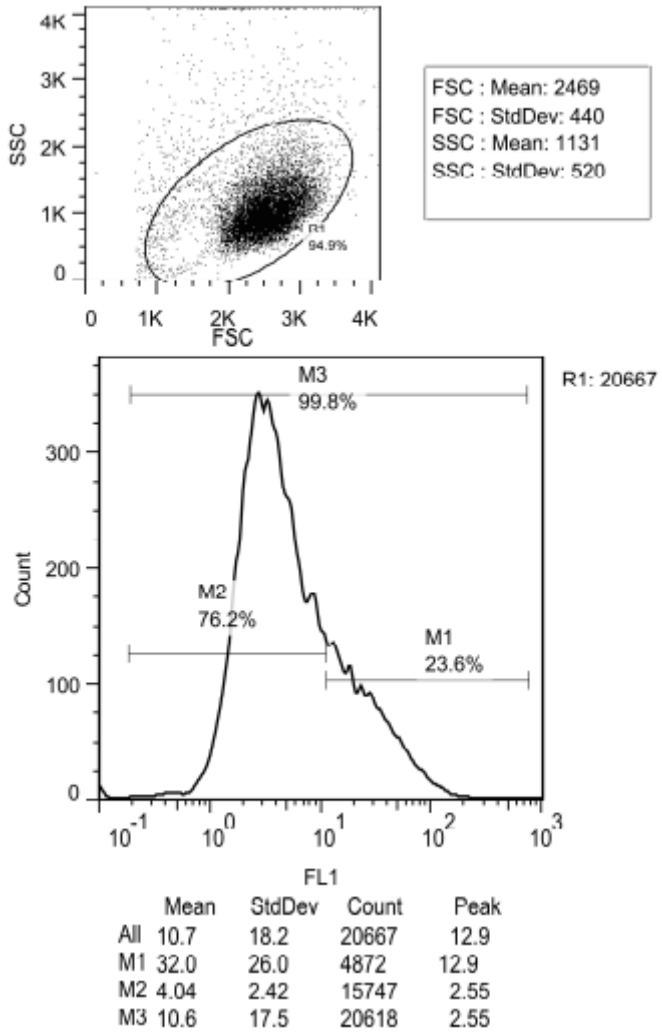

Figure S35: Flow cytometry data for compound **6** tested at 0.2 µM in resistant human *ABCB1*-gene transfected L5178Y subline (MDR)

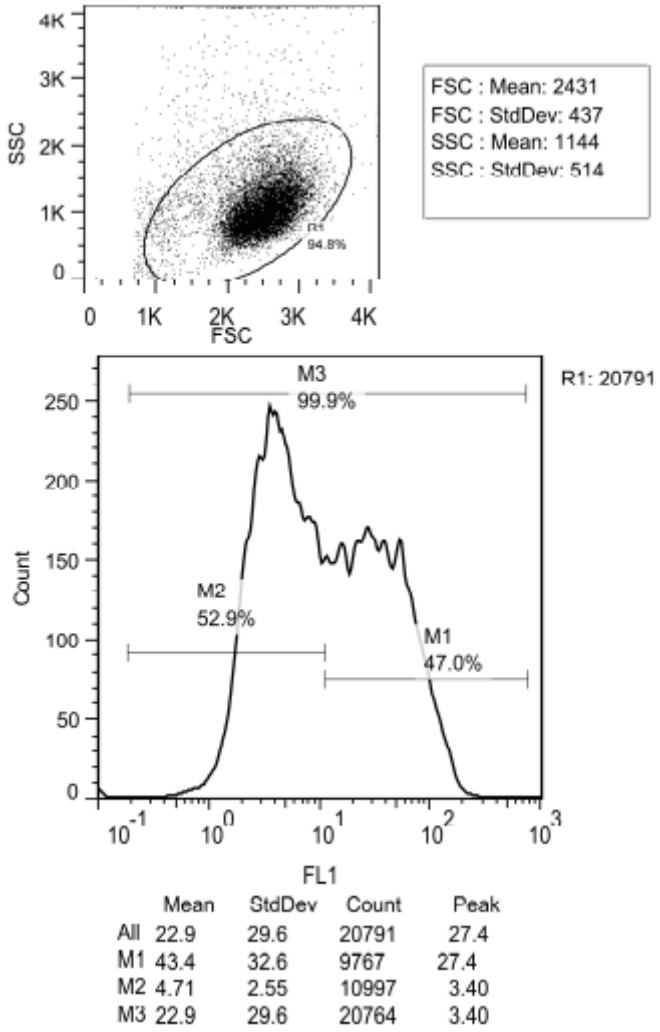

Figure S36: Flow cytometry data for compound **6** tested at 2 µM in resistant human *ABCB1*-gene transfected L5178Y subline (MDR)

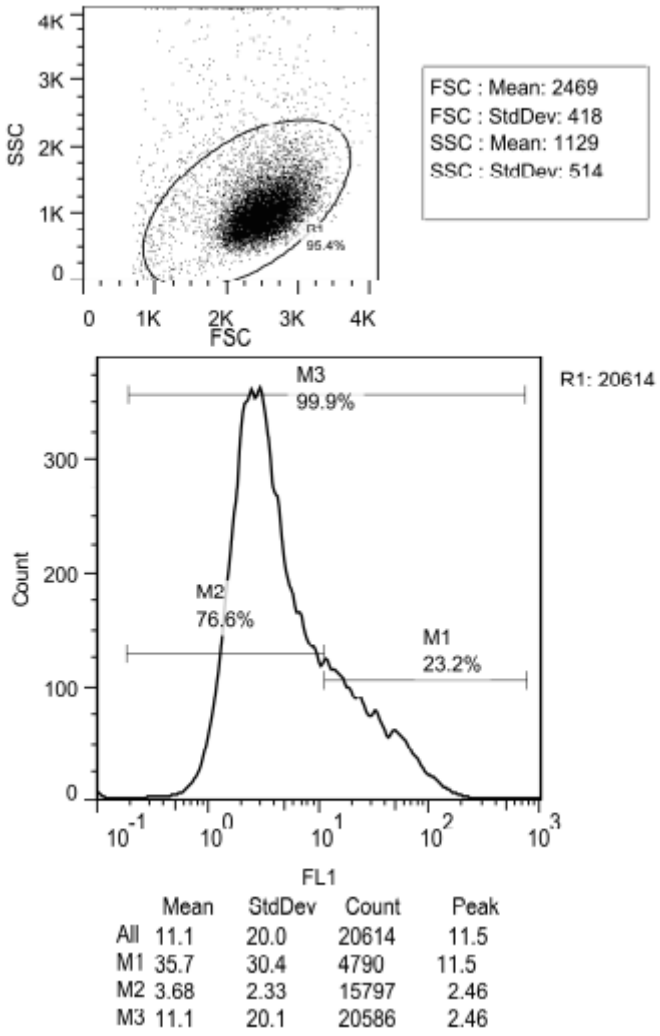

Figure S37: Flow cytometry data for compound **7** tested at 0.2 µM in resistant human *ABCB1*-gene transfected L5178Y subline (MDR)

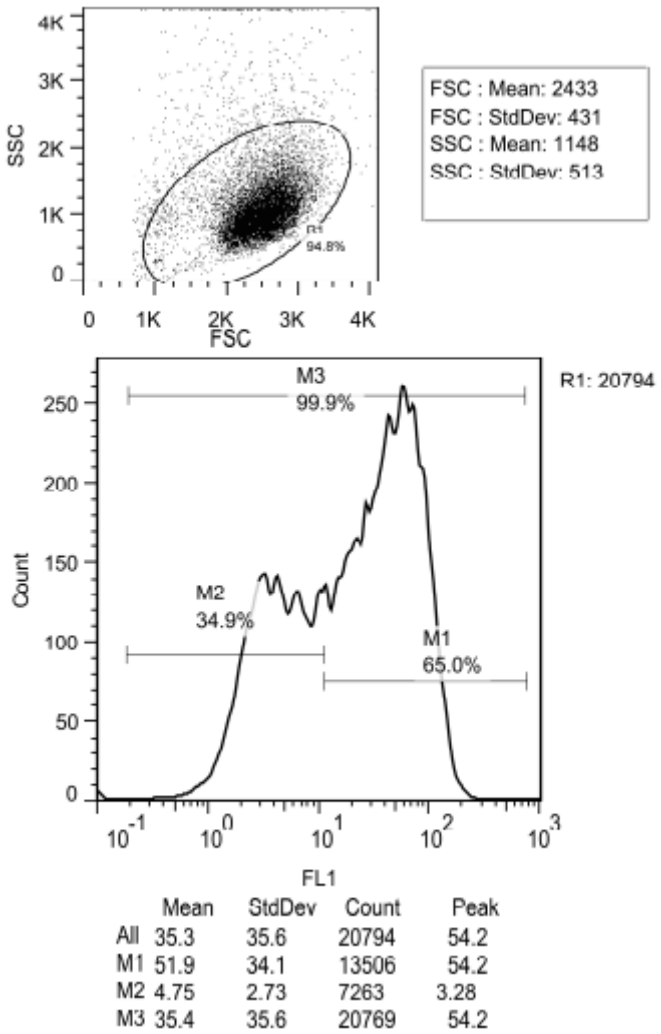

Figure S38: Flow cytometry data for compound **7** tested at 2 µM in resistant human *ABCB1*-gene transfected L5178Y subline (MDR)

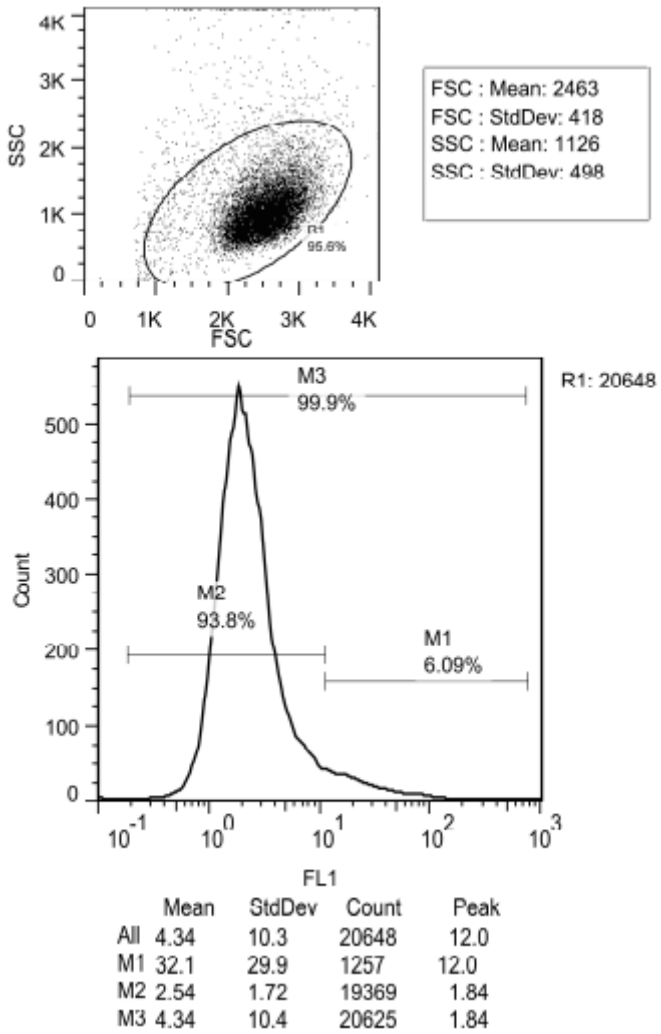

Figure S39: Flow cytometry data for compound **8** tested at 0.2 µM in resistant human *ABCB1*-gene transfected L5178Y subline (MDR)

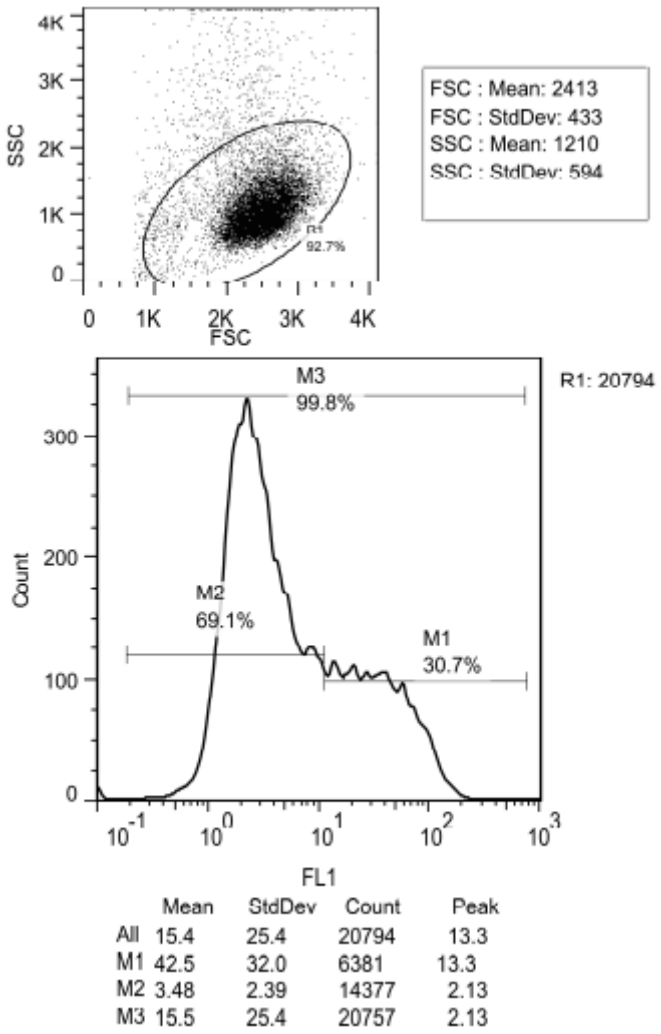

Figure S40: Flow cytometry data for compound **8** tested at 2 µM in resistant human *ABCB1*-gene transfected L5178Y subline (MDR)

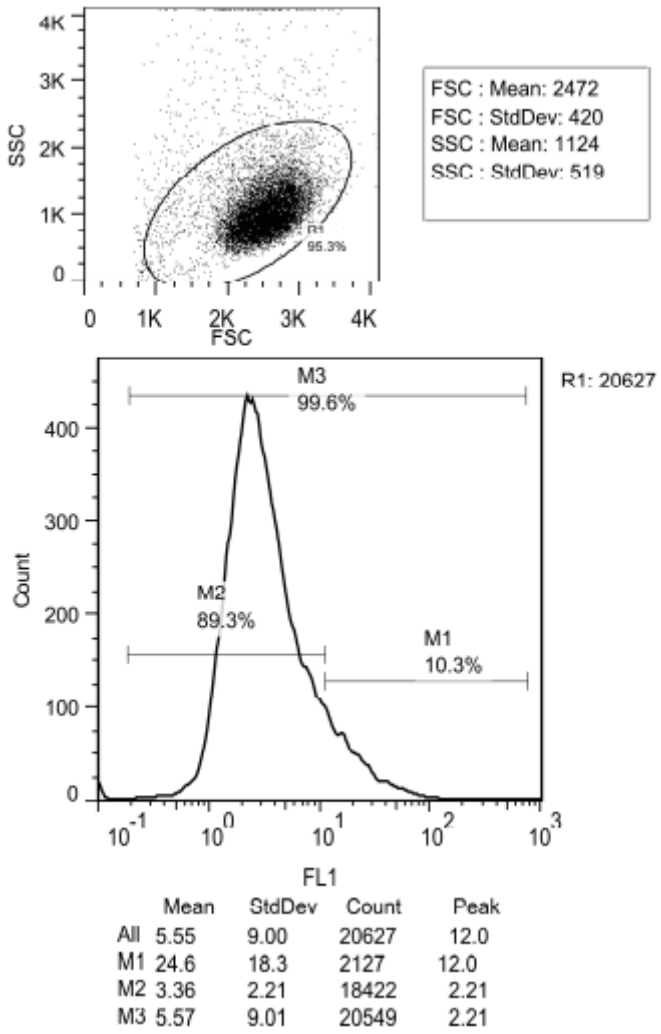

Figure S41: Flow cytometry data for compound **9** tested at 0.2 µM in resistant human *ABCB1*-gene transfected L5178Y subline (MDR)

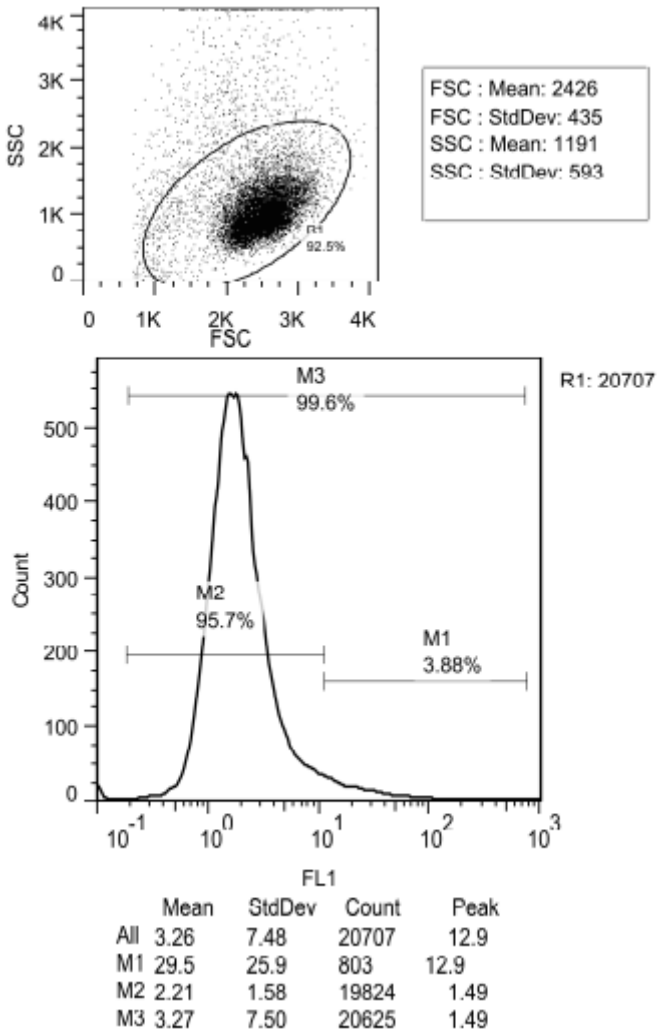

Figure S42: Flow cytometry data for compound **9** tested at 2 µM in resistant human *ABCB1*-gene transfected L5178Y subline (MDR)

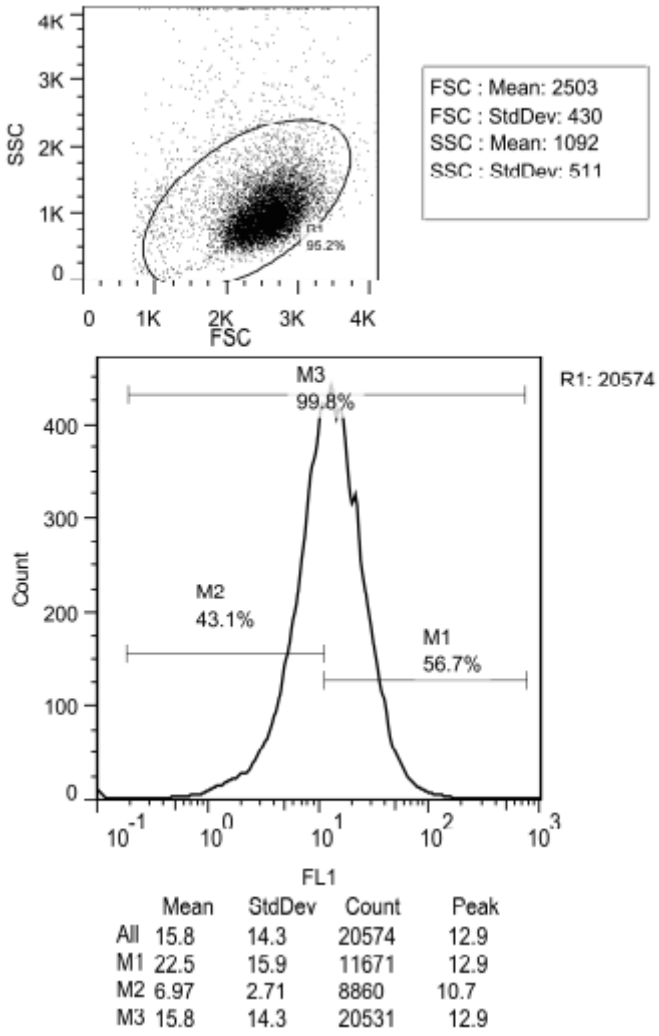

Figure S43: Flow cytometry data for compound **10** tested at 0.2 µM in resistant human *ABCB1*-gene transfected L5178Y subline (MDR)

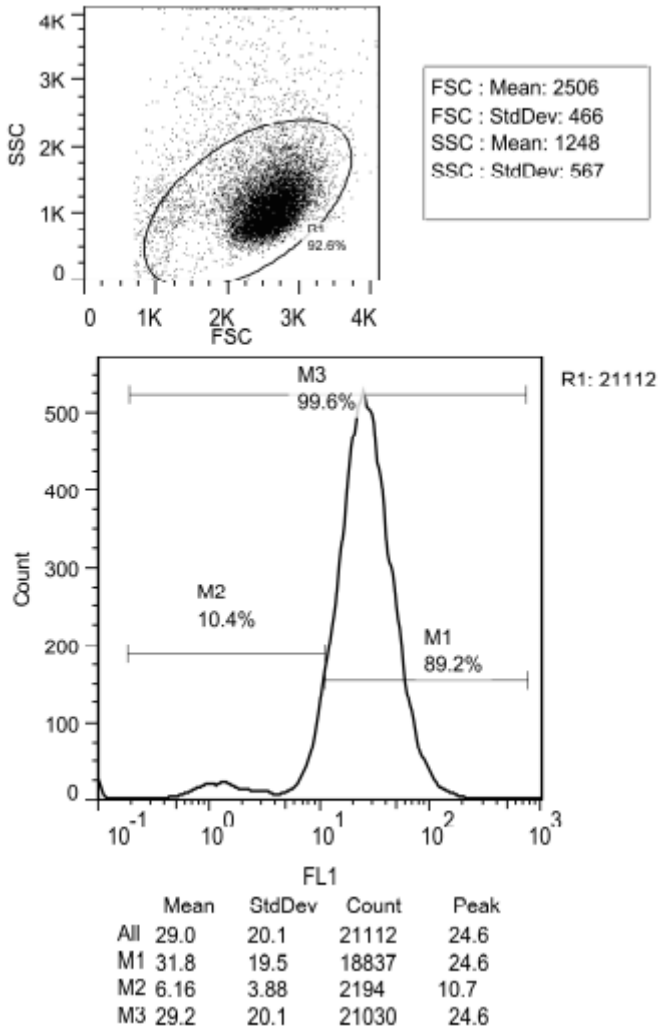

	Mean	StdDev	Count	Peak
All	29.0	20.1	21112	24.6
M1	31.8	19.5	18837	24.6
M2	6.16	3.88	2194	10.7
M3	29.2	20.1	21030	24.6

Figure S44: Flow cytometry data for compound **10** tested at 2 µM in resistant human *ABCB1*-gene transfected L5178Y subline (MDR)

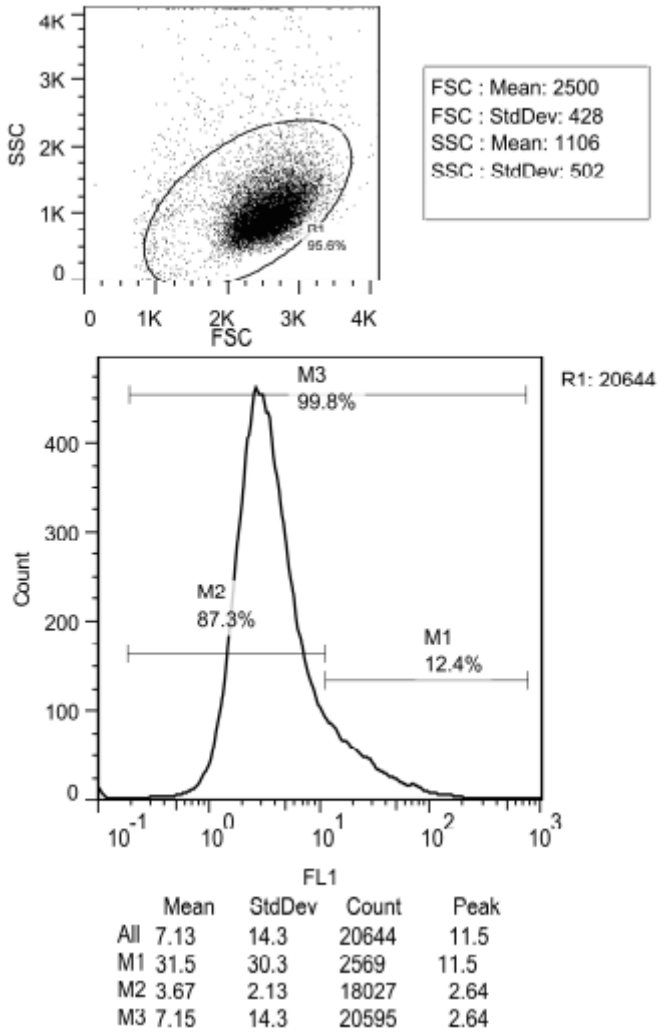

Figure S45: Flow cytometry data for compound **11** tested at 0.2 µM in resistant human *ABCB1*-gene transfected L5178Y subline (MDR)

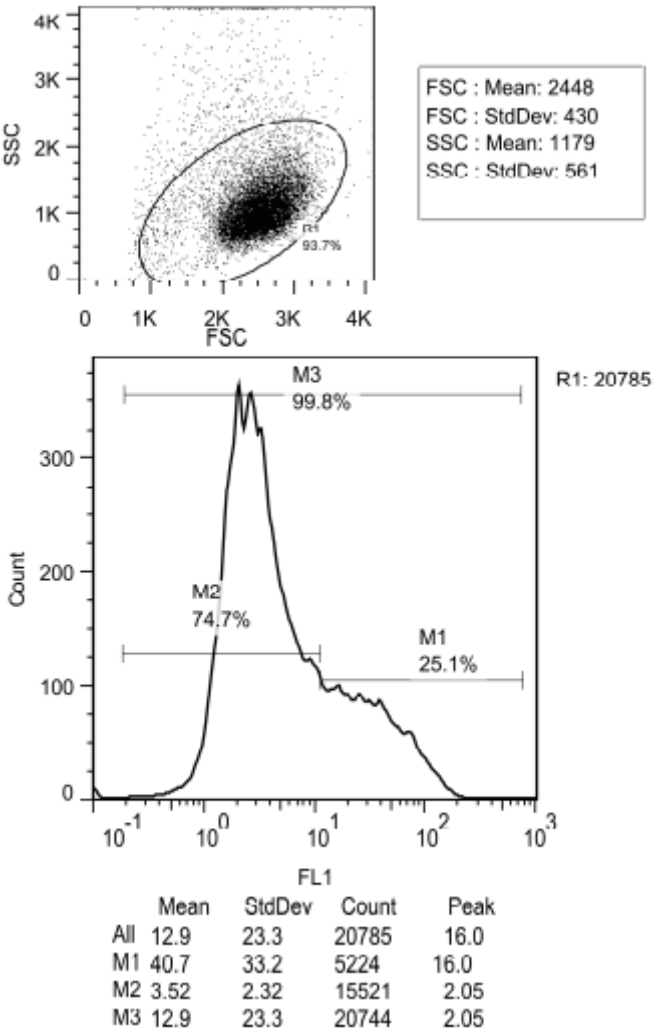

Figure S46: Flow cytometry data for compound **11** tested at 2 µM in resistant human *ABCB1*-gene transfected L5178Y subline (MDR)

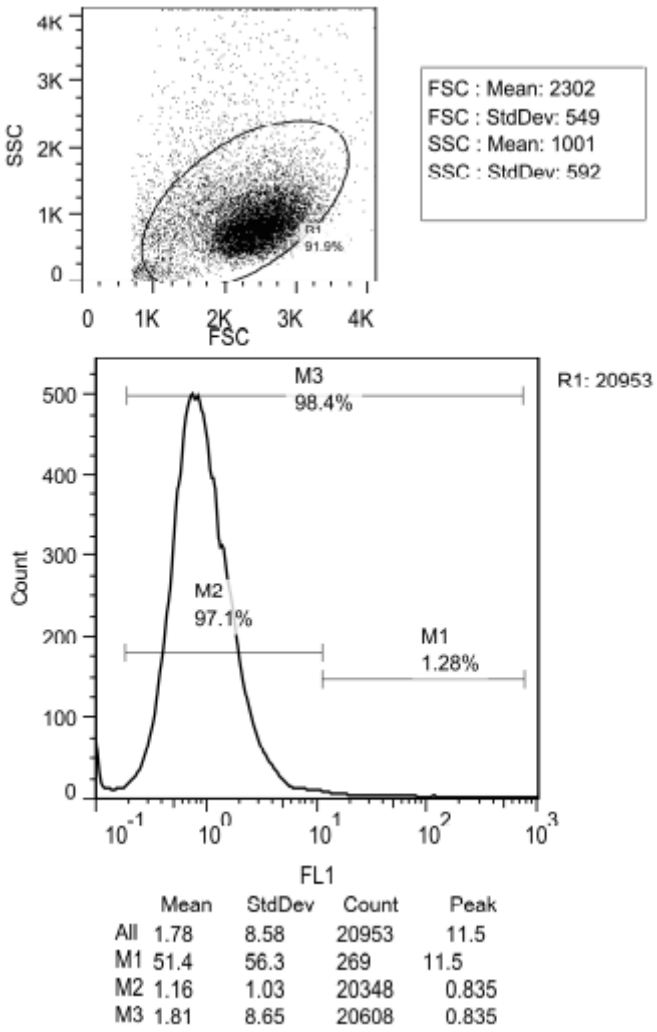

Figure S47: Flow cytometry data for compound **12** tested at 2 µM in resistant human *ABCB1*-gene transfected L5178Y subline (MDR)

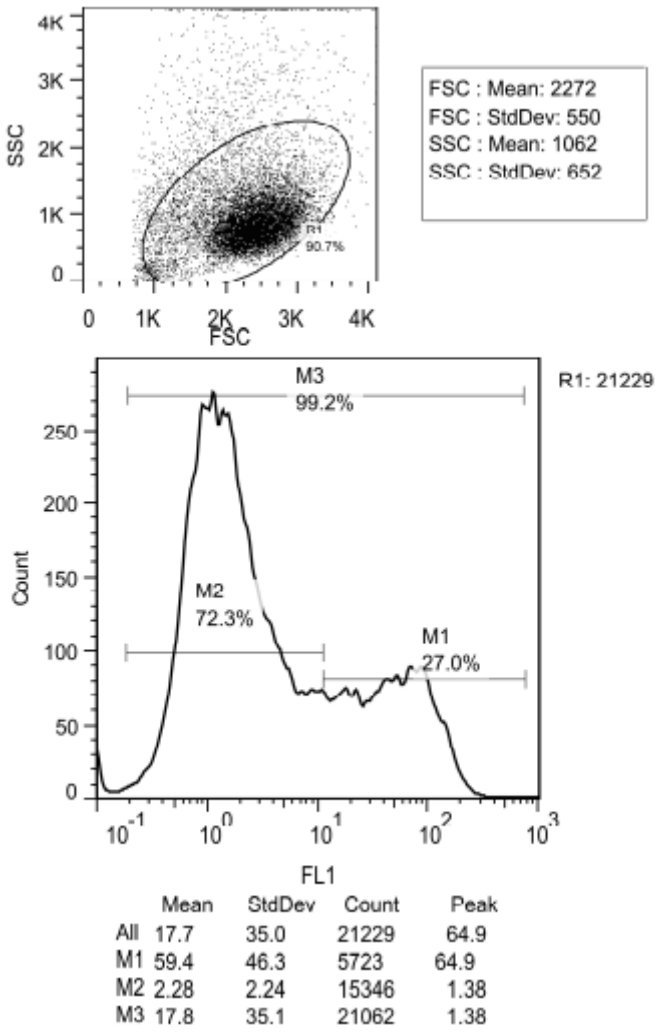

Figure S48: Flow cytometry data for compound **12** tested at 20 µM in resistant human *ABCB1*-gene transfected L5178Y subline (MDR)

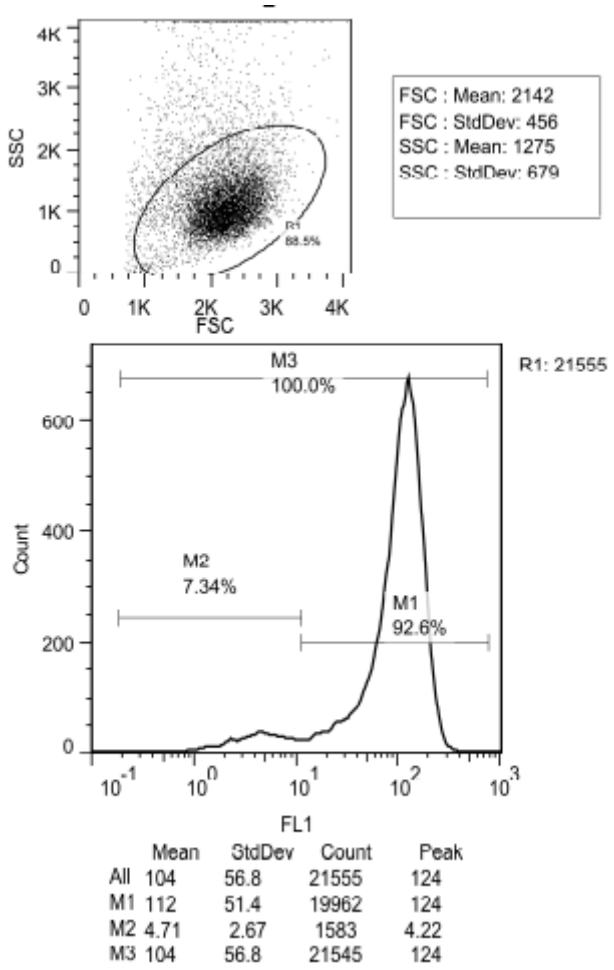

Figure S49: Flow cytometry data for compound **13** tested at 2 µM in resistant human *ABCB1*-gene transfected L5178Y subline (MDR)

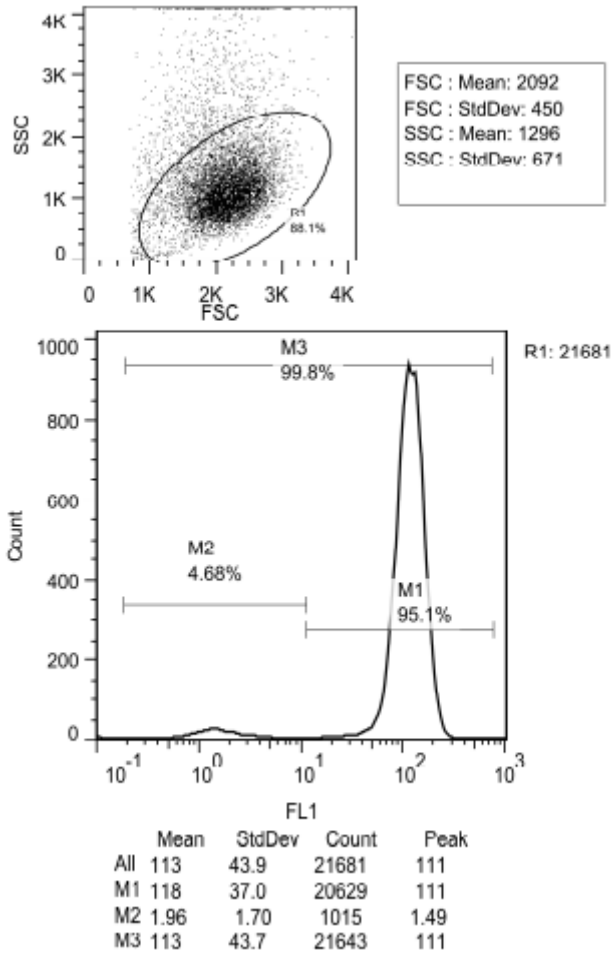

Figure S50: Flow cytometry data for compound **13** tested at 20 µM in resistant human *ABCB1*-gene transfected L5178Y subline (MDR)

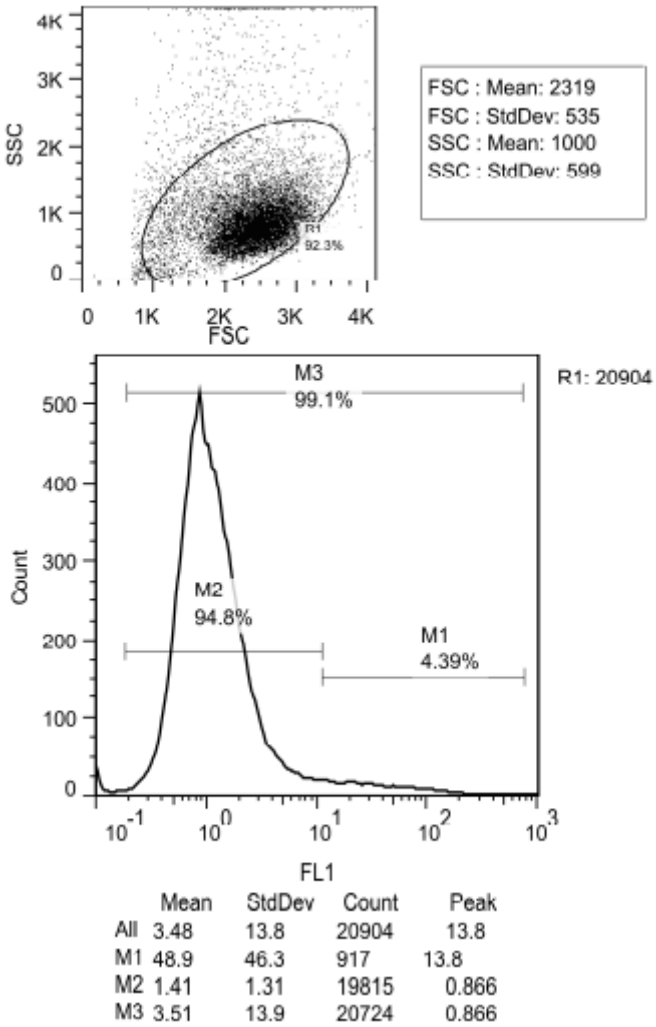

Figure S51: Flow cytometry data for compound **14** tested at 2 µM in resistant human *ABCB1*-gene transfected L5178Y subline (MDR)

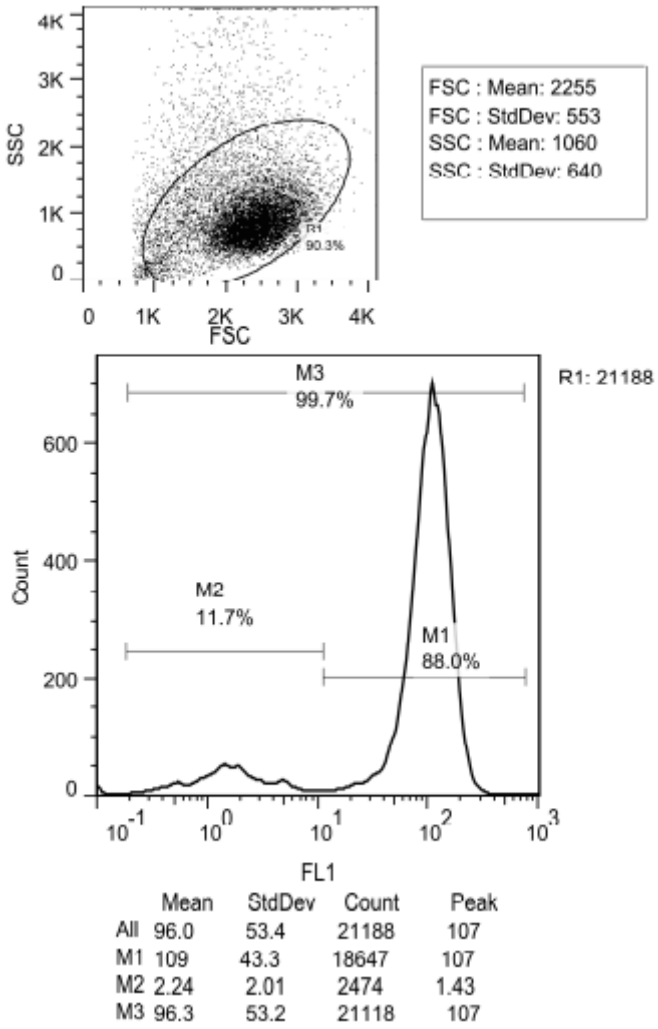

Figure S52: Flow cytometry data for compound **14** tested at 20 µM in resistant human *ABCB1*-gene transfected L5178Y subline (MDR)

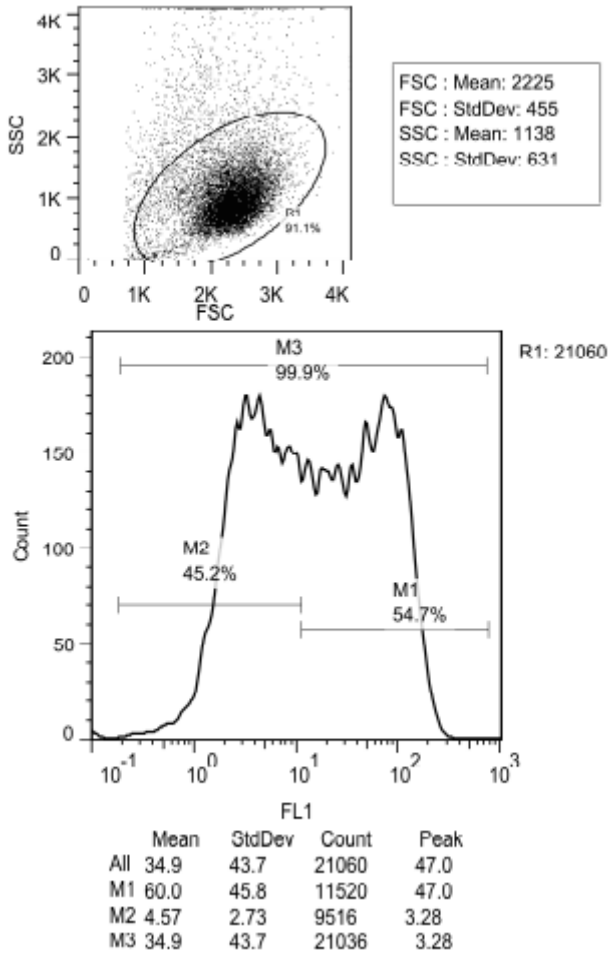

Figure S53: Flow cytometry data for compound **15** tested at 2 µM in resistant human *ABCB1*-gene transfected L5178Y subline (MDR)

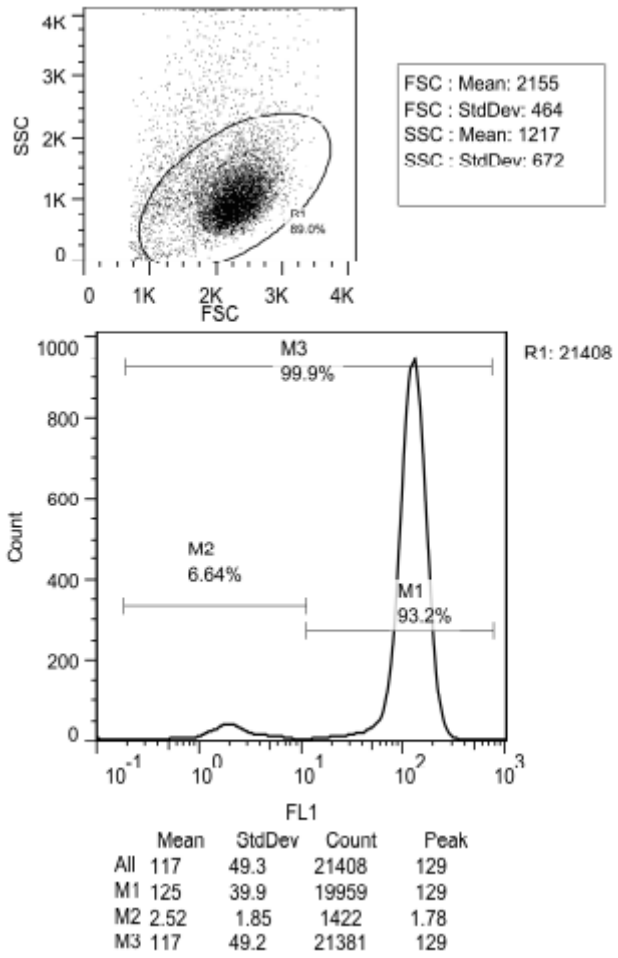

Figure S54: Flow cytometry data for compound **15** tested at 20 µM in resistant human *ABCB1*-gene transfected L5178Y subline (MDR)

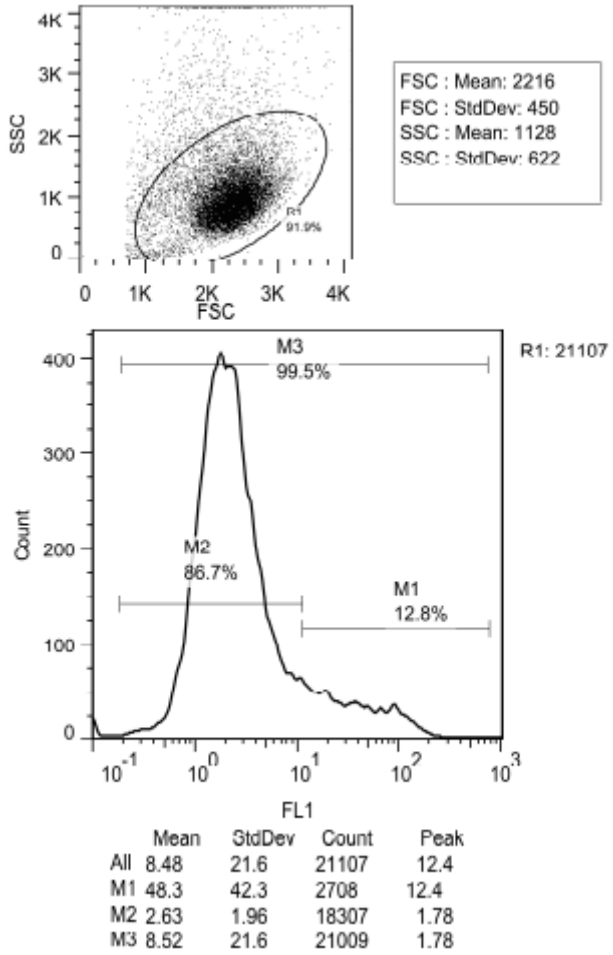

Figure S55: Flow cytometry data for compound **16** tested at 2 µM in resistant human *ABCB1*-gene transfected L5178Y subline (MDR)

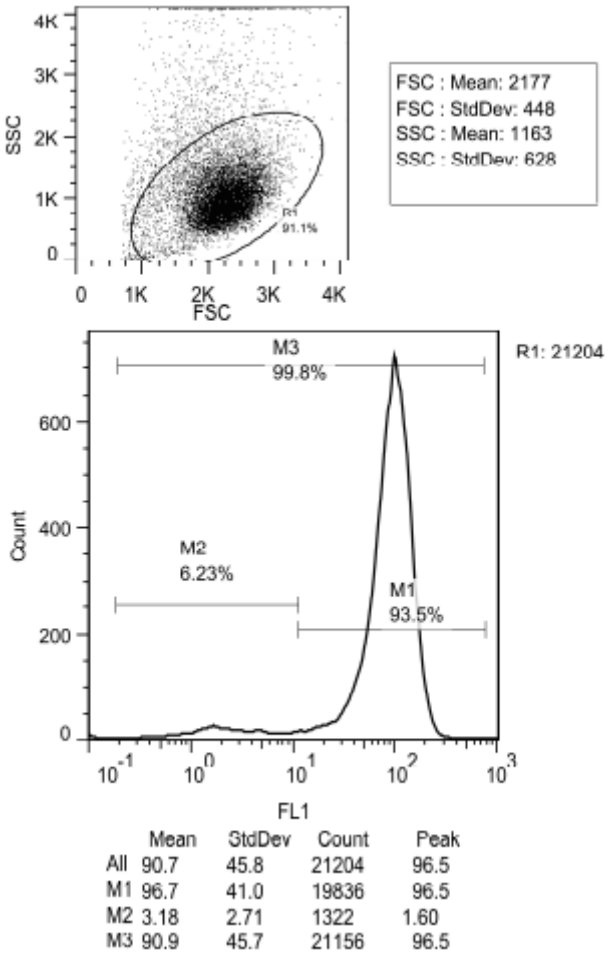

Figure S56: Flow cytometry data for compound **16** tested at 20 µM in resistant human *ABCB1*-gene transfected L5178Y subline (MDR)

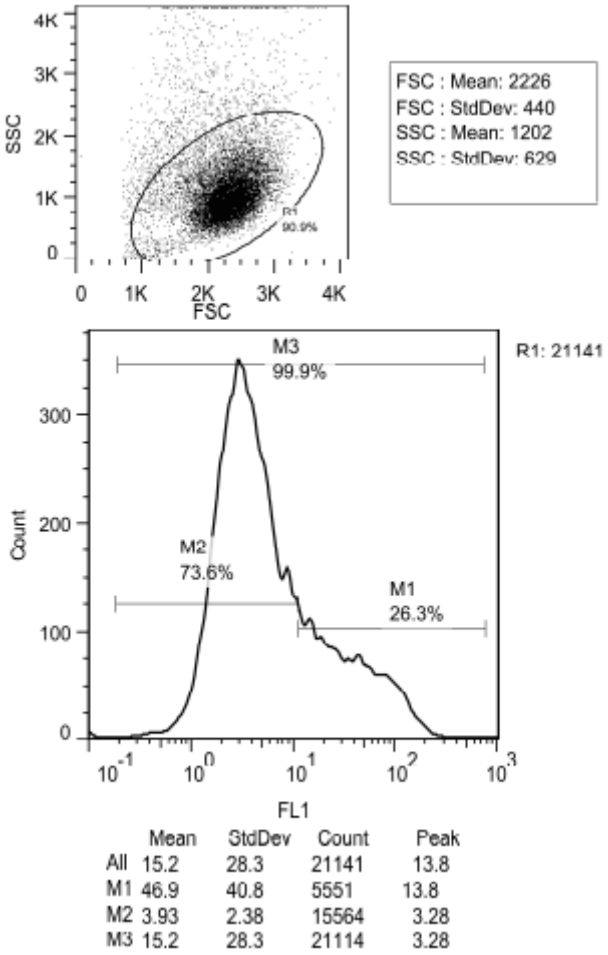

Figure S57: Flow cytometry data for compound **17** tested at 2 µM in resistant human *ABCB1*-gene transfected L5178Y subline (MDR)

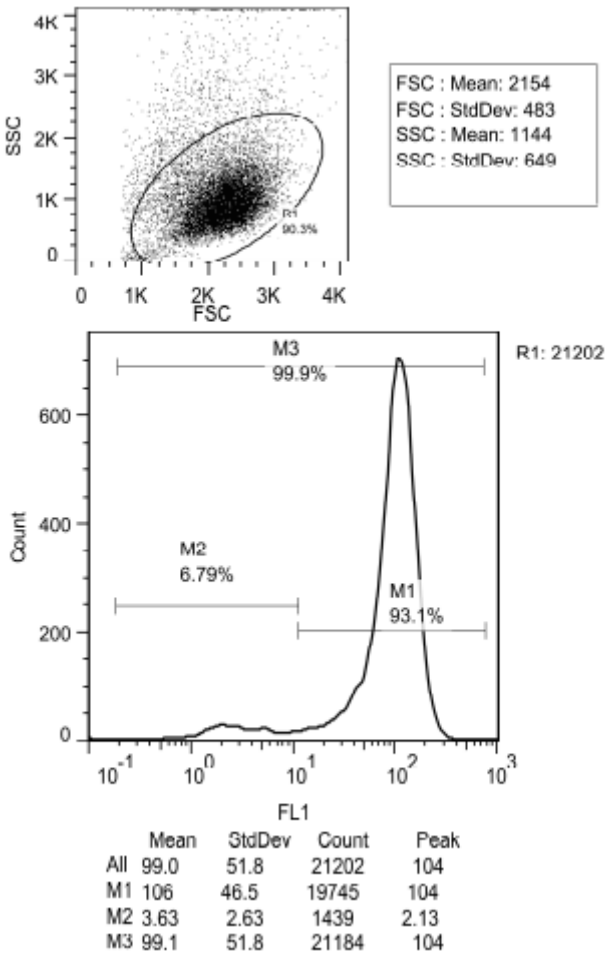

Figure S58: Flow cytometry data for compound **17** tested at 20 µM in resistant human *ABCB1*-gene transfected L5178Y subline (MDR)

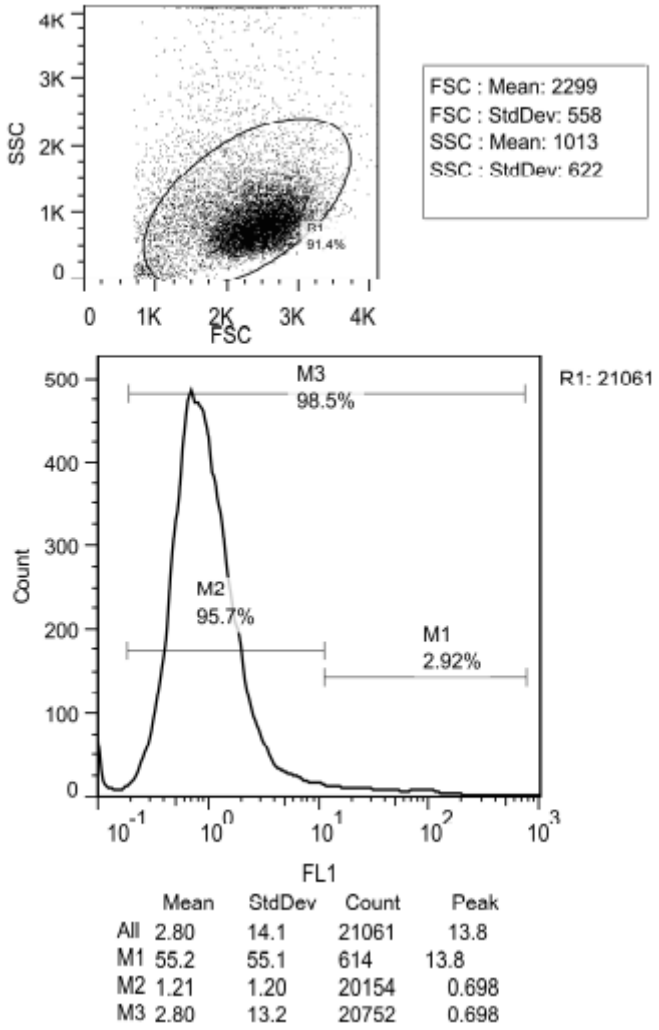

Figure S59: Flow cytometry data for compound **18** tested at 2 µM in resistant human *ABCB1*-gene transfected L5178Y subline (MDR)

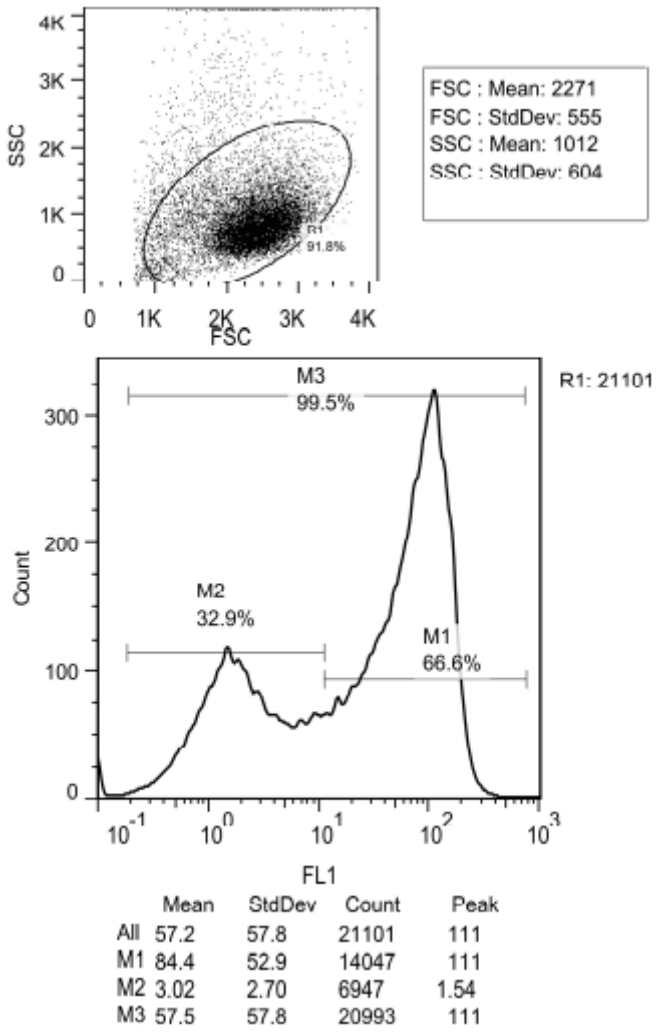

Figure S60: Flow cytometry data for compound **18** tested at 20 µM in resistant human *ABCB1*-gene transfected L5178Y subline (MDR)

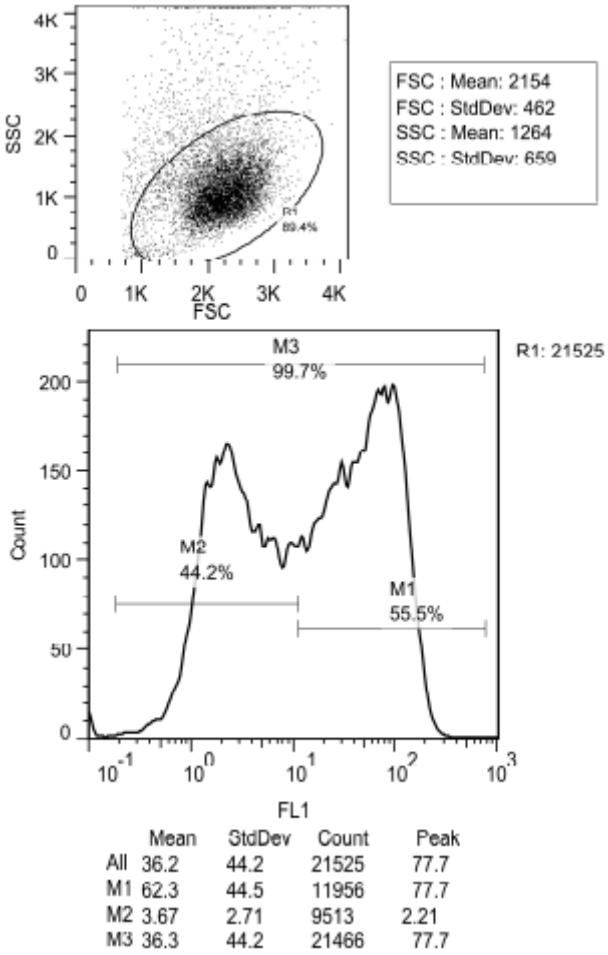

Figure S61: Flow cytometry data for compound **19** tested at 2 µM in resistant human *ABCB1*-gene transfected L5178Y subline (MDR)

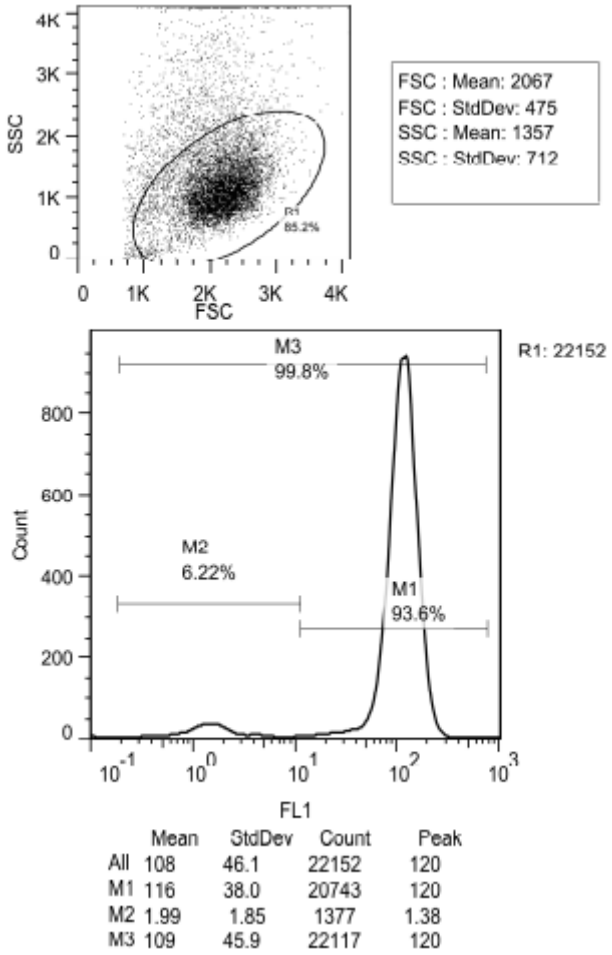

Figure S62: Flow cytometry data for compound **19** tested at 20 µM in resistant human *ABCB1*-gene transfected L5178Y subline (MDR)

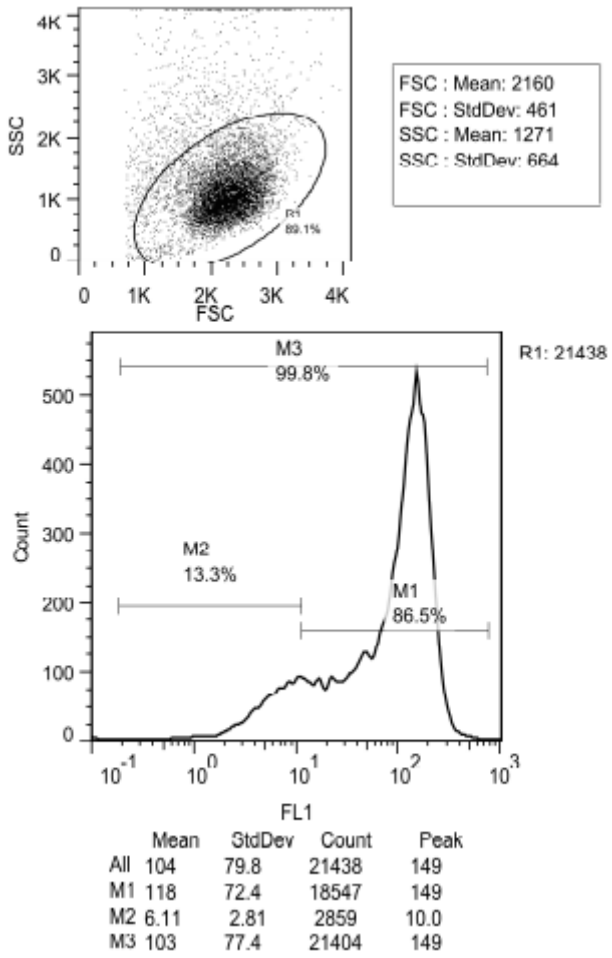

Figure S63: Flow cytometry data for compound **20** tested at 2 µM in resistant human *ABCB1*-gene transfected L5178Y subline (MDR)

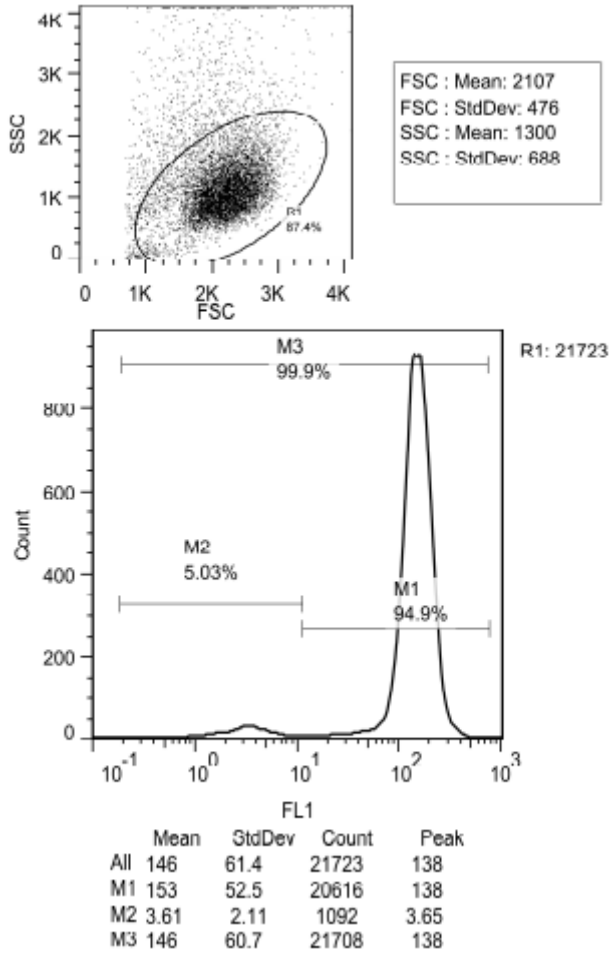

Figure S64: Flow cytometry data for compound **20** tested at 2 µM in resistant human *ABCB1*-gene transfected L5178Y subline (MDR)

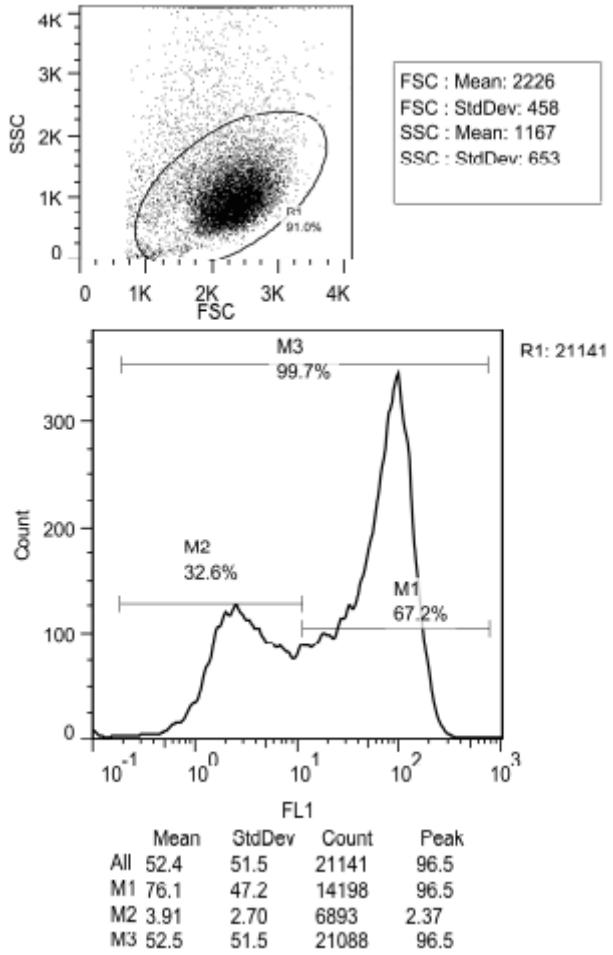

Figure S65: Flow cytometry data for compound **21** tested at 2 µM in resistant human *ABCB1*-gene transfected L5178Y subline (MDR)

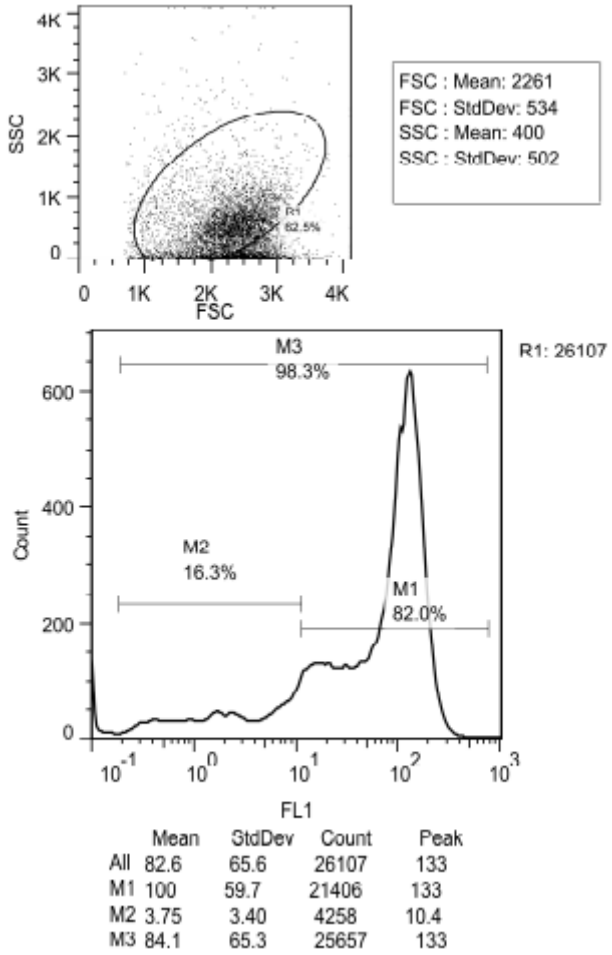

Figure S66: Flow cytometry data for compound **21** tested at 20 µM in resistant human *ABCB1*-gene transfected L5178Y subline (MDR)

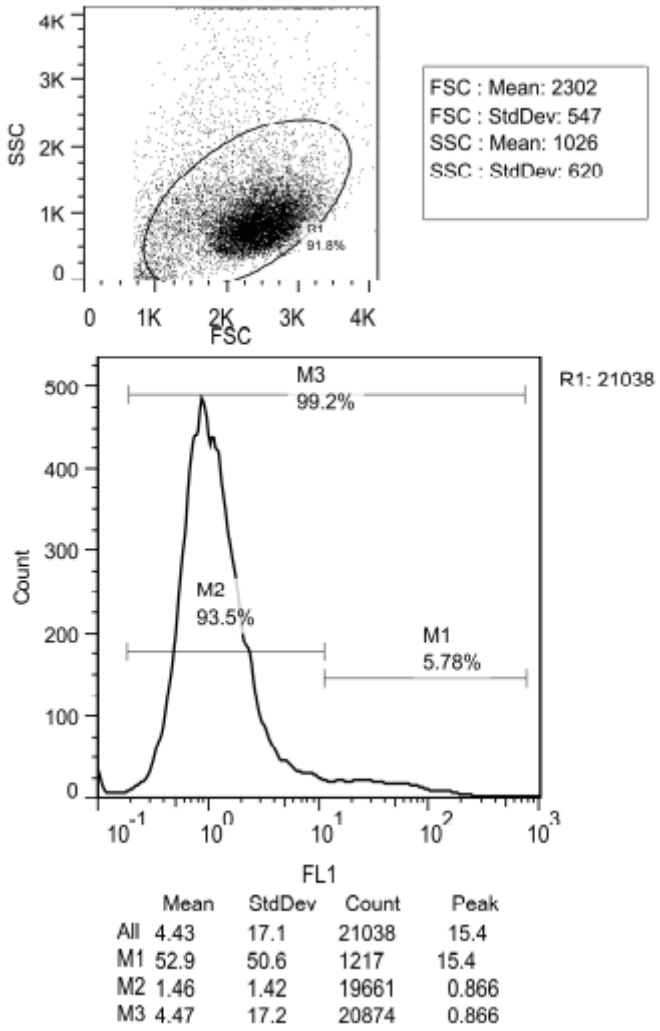

Figure S67: Flow cytometry data for compound **22** tested at 2 µM in resistant human *ABCB1*-gene transfected L5178Y subline (MDR)

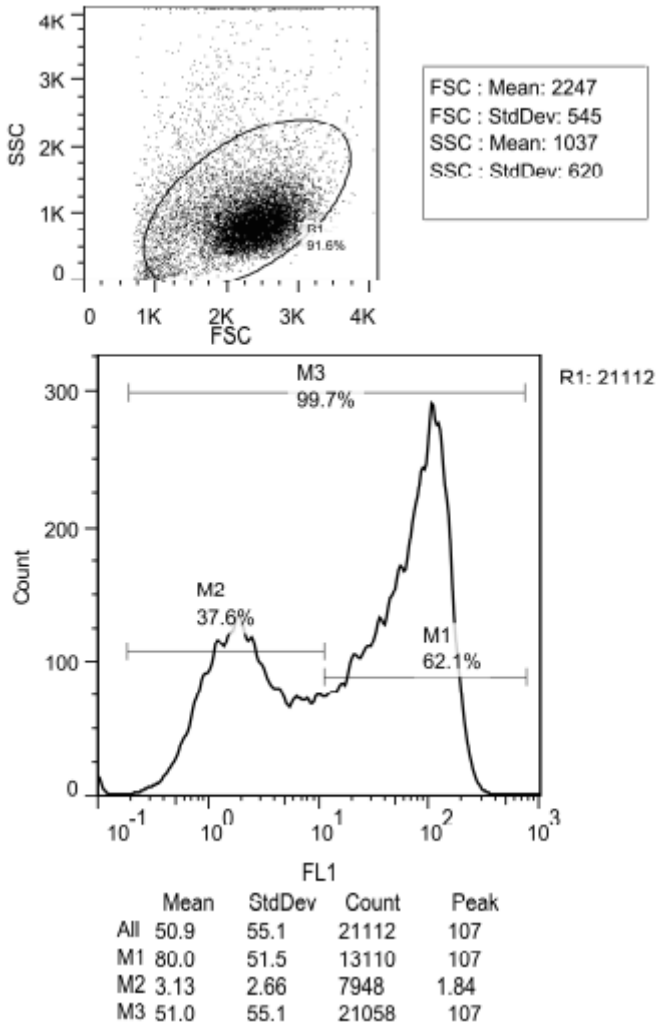

Figure S68: Flow cytometry data for compound **22** tested at 20 µM in resistant human *ABCB1*-gene transfected L5178Y subline (MDR)

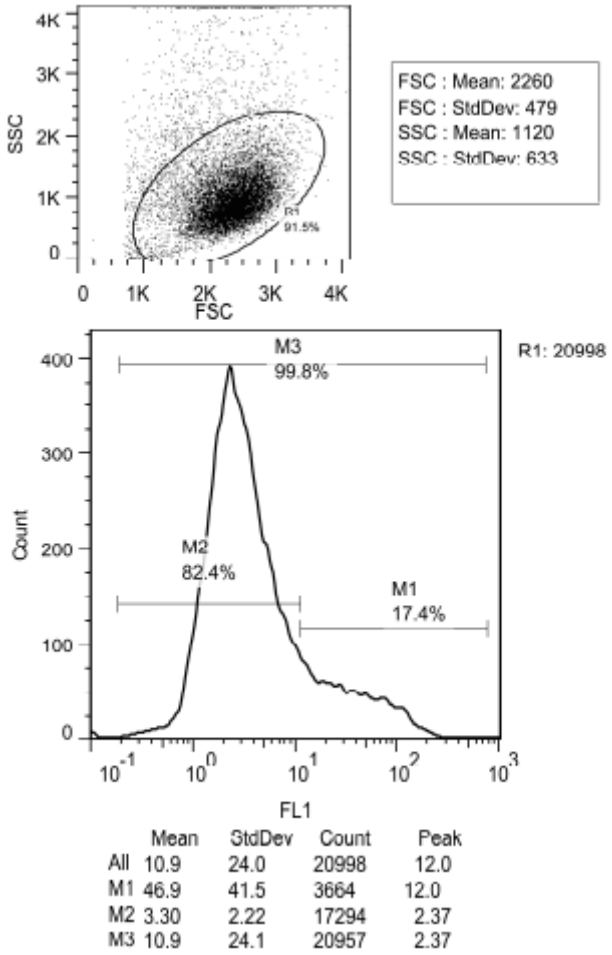

Figure S69: Flow cytometry data for compound **23** tested at 2 µM in resistant human *ABCB1*-gene transfected L5178Y subline (MDR)

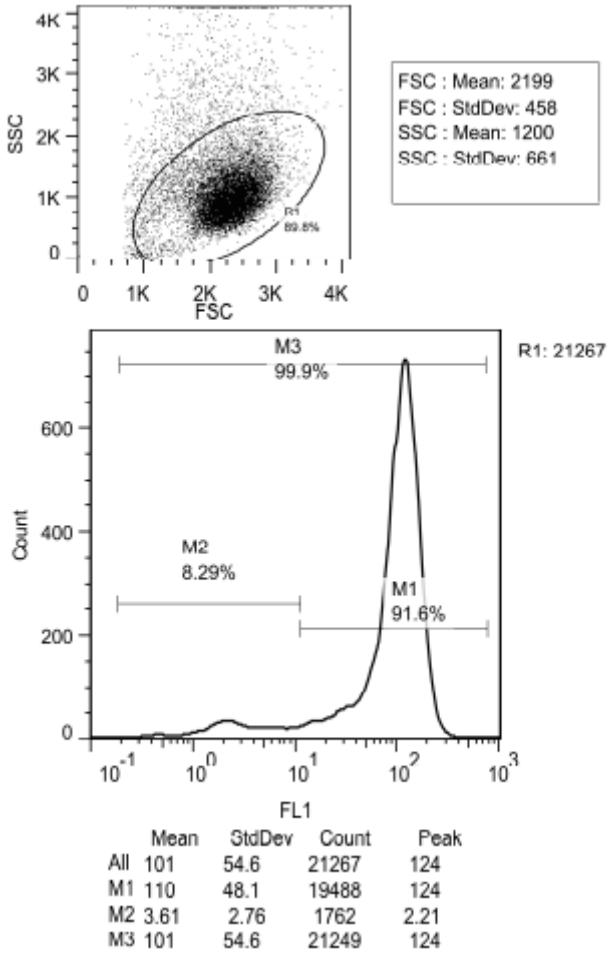

Figure S70: Flow cytometry data for compound **23** tested at 20 µM in resistant human *ABCB1*-gene transfected L5178Y subline (MDR)

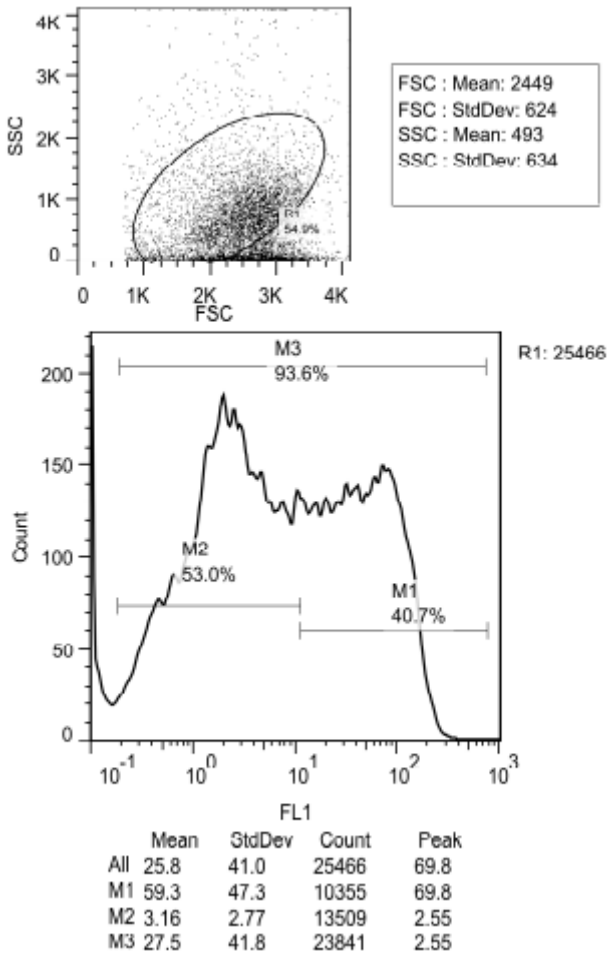

Figure S71: Flow cytometry data for compound **24** tested at 2 µM in resistant human *ABCB1*-gene transfected L5178Y subline (MDR)

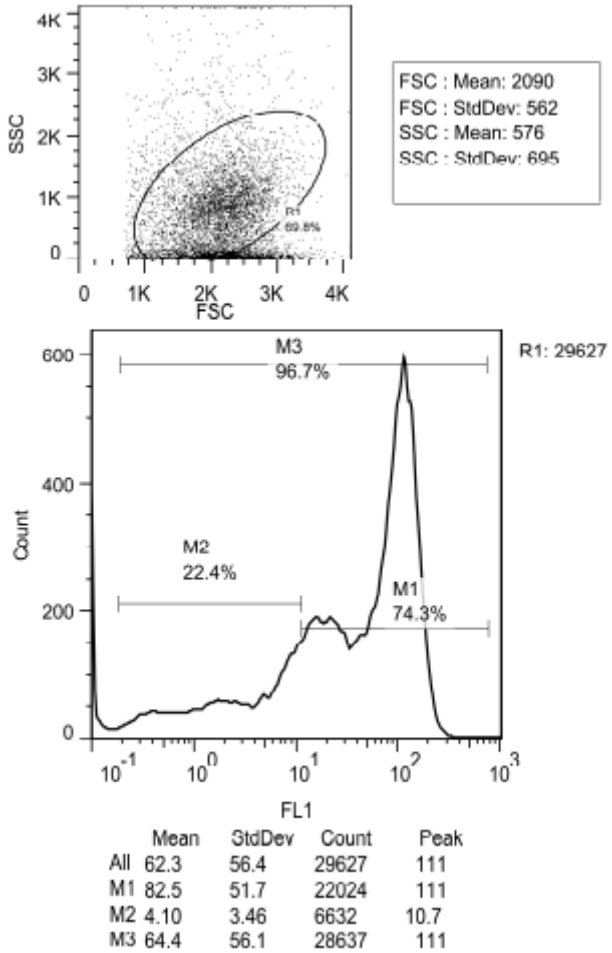

Figure S72: Flow cytometry data for compound **24** tested at 20 µM in resistant human *ABCB1*-gene transfected L5178Y subline (MDR)

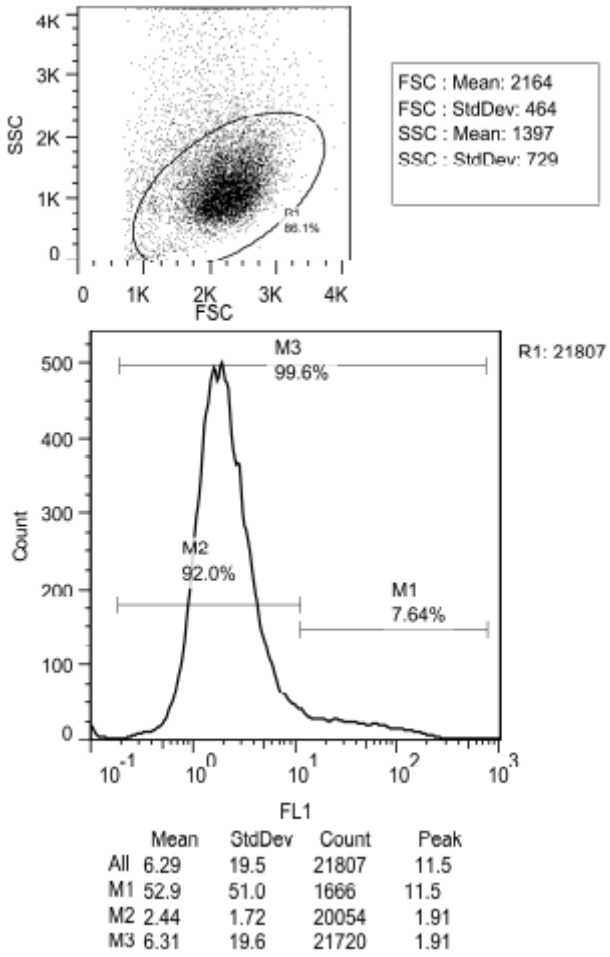

Figure S73: Flow cytometry data for compound **25** tested at 2 µM in resistant human *ABCB1*-gene transfected L5178Y subline (MDR)

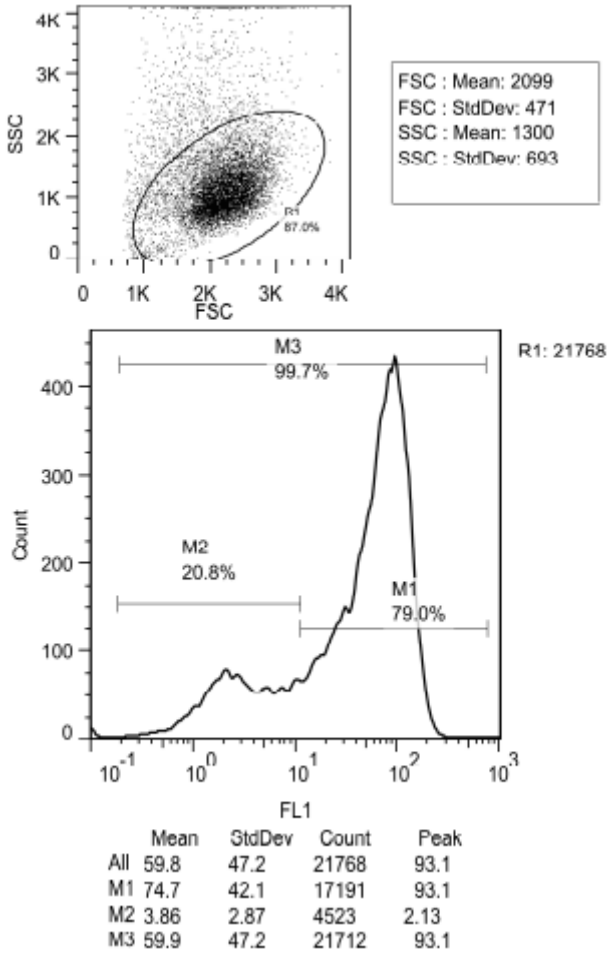

Figure S74: Flow cytometry data for compound **25** tested at 20 µM in resistant human *ABCB1*-gene transfected L5178Y subline (MDR)

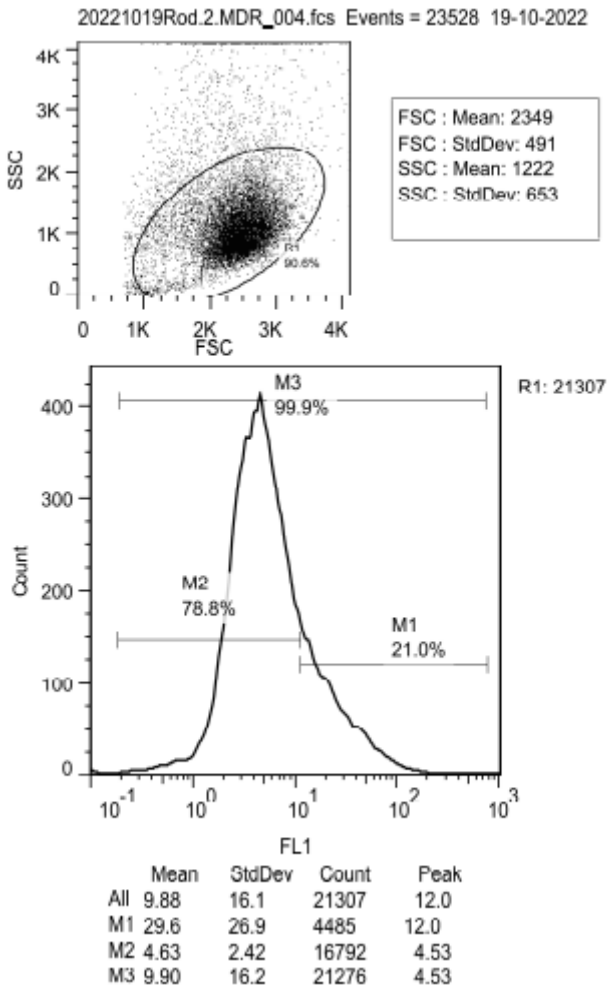

Figure S75: Flow cytometry data for verapamil tested at 20 µM in resistant human *ABCB1*-gene transfected L5178Y subline (MDR)

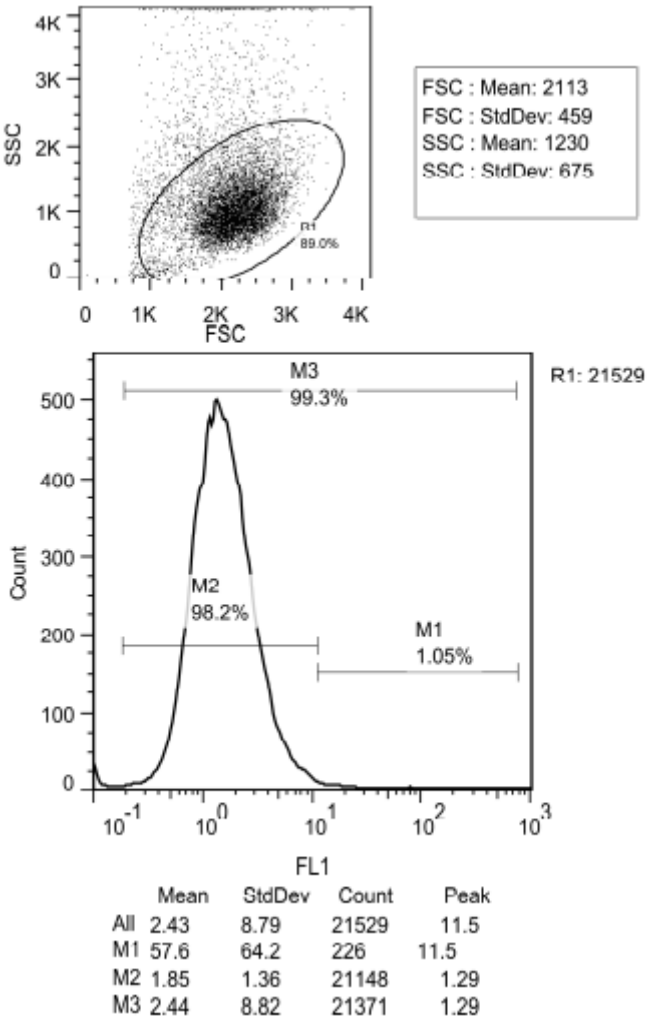

Figure S75: Flow cytometry data for dimethylsulfoxide tested at 2 % in resistant human *ABCB1*-gene transfected L5178Y subline (MDR)

5. Combination chemotherapy results

Table S2: Effect of compounds **1-11** in combination with doxorubicin on resistant human *ABCB1*-gene transfected L5178Y subline (MDR)

Compound	Starting Conc. (μM)	Ratio*	R	CI at ED_{50}	SD	Type of interaction
1	30	1:6.96	0.997	0.98	0.15	Nearly additive
2	38	1:71.41	1.0	1.60	0.21	Antagonism
3	24	1:44.56	1.0	0.21	0.12	Strong synergism
4	47	1:10.9	0.976	0.37	0.05	Synergism
5	11	1:2.55	0.998	0.71	0.11	Moderate synergism
6	18	1:16.72	0.995	0.55	0.11	Synergism
7	30	1:14.14	0.995	0.52	0.05	Synergism
8	24	1:5.45	0.993	0.56	0.80	Synergism
9	24	1:21.8	0.994	0.60	0.06	Synergism
10	30	1:14.14	0.997	0.60	0.04	Synergism
11	30	1:27.84	1.0	0.75	0.08	Moderate synergism

*Ratio: the applied combination and concentration of amine derivatives and doxorubicin (the best combination ratio between compound and doxorubicin). R: Linear Correlation Coefficient. CI at ED_{50}: combination index (CI) at the 50 % growth inhibition dose; CI < 0.1: very strong synergism; 0.1 < CI < 0.3: strong synergism; 0.3 < CI < 0.7: synergism; 0.7 < CI < 0.9: moderate to slight synergism; 0.9 < CI < 1.1: nearly additive; 1.10 < CI < 1.45: moderate antagonism; 1.45 < CI < 3.30: antagonism.

6. Physicochemical properties

Table S3 - *In silico* molecular properties of compounds **1-25** and verapamil using the SwissADME predictive database.[a.]

Compound	Descriptors				
	Molecular weight (g/mol)	**LogP**	**HBD**	**HBA**	**TPSA**
1	350.45	2.33	3	5	86.99
2	476.56	3.53	0	8	105.2
3	604.53	4.64	2	8	115.85
4	612.71	4.35	2	10	138.49
5	567.67	3.57	3	8	146.05
6	587.10	4.59	2	8	120.03
7	620.66	5.20	2	11	120.03
8	620.66	4.92	2	11	120.03
9	556.65	3.22	2	9	132.92
10	542.62	3.61	2	9	133.17
11	558.69	4.28	2	8	148.27
12	521.67	3.25	3	7	147.08
13	535.70	3.45	2	7	138.29
14	563.75	4.25	3	7	147.08
15	589.79	4.47	3	7	147.08
16	620.80	3.28	3	9	159.55

Table S3: Continuation

Compound	Descriptors				
	Molecular weight (g/mol)	LogP	HBD	HBA	TPSA
17	583.74	4.41	3	7	147.08
18	597.77	4.69	3	7	147.08
19	597.77	4.79	3	7	147.08
20	611.79	5.10	3	7	147.08
21	628.74	3.78	9	3	192.90
22	601.73	4.87	3	8	147.08
23	597.77	4.60	3	7	147.08
24	633.80	5.38	3	7	147.08
25	687.73	3.91	3	8	160.22
Verapamil	440.58	4.29	3	9	72.74

Octanol-water partition coefficient *(*LogP); number of hydrogen bond acceptors (HBA); number of hydrogen bond donors (HBD); topological polar surface area (TPSA); Lipinski's rule of five: molecular weight < 500 Da; Log P < 5; HBA< 5; HBD < 10. A maximum of 1 violation is permitted.

Table S4: *In silico* pharmacokinetic (absorption, distribution, metabolism, and excretion) and toxicity parameters of compounds **1-25** and verapamil using pkCSM and SwissADME predictive databases.

Compound	Log S (mol/L)	Caco-2 Permeability (log Papp in 10^{-6} cm/S	Intestinal Absorption (%)	Fractional unbound (fu)	CNS permeability (logPS)	CYP3A4 inhibitor (Yes/No)	Hepato toxicity	AMES toxicity
1	-3.10	1.35	95.36	0.20	-2.47	No	No	No
2	-5.03	0.93	90.04	0.09	-2.59	Yes	No	No
3	-5.15	0.66	86.66	0.05	-2.74	Yes	Yes	No
4	-5.85	0.35	82.28	0	-3.03	Yes	Yes	No
5	-4.92	0.02	76.54	0.13	-2.84	Yes	Yes	No
6	-5.62	0.80	84.80	0	-2.65	Yes	No	No
7	-5.71	0.81	85.94	0	-2.64	Yes	Yes	No
8	-5.71	0.81	85.91	0	-2.63	Yes	Yes	No
9	-5.05	0.75	79.14	0.05	-2.95	Yes	Yes	No
10	-4.73	0.68	82.88	0.11	-2.90	Yes	Yes	No
11	-5.24	0.88	83.97	0	-2.76	Yes	Yes	No
12	-4.43	0.78	70.34	0.20	-3.07	No	No	No
13	-4.59	0.83	71.06	0.18	-3.02	No	Yes	No
14	-4.57	0.90	73.68	0.06	-2.81	No	Yes	No
15	-5.04	0.76	78.64	0.10	-2.90	No	Yes	No
16	-4.15	0.73	64.04	0.31	-3.39	No	Yes	No
17	-4.92	0.89	79.83	0.04	-2.68	No	Yes	No
18	-4.98	0.89	80.29	0.03	-2.63	No	No	No
19	-4.98	0.79	80.28	0.01	-2.63	No	Yes	No
20	-5.07	0.82	80.36	0.02	-2.64	Yes	No	No
21	-4.85	-0.27	76.62	0.06	-2.84	Yes	Yes	No
22	-4.92	0.89	80.17	0.05	-2.74	No	No	No
23	-5.32	0.87	77.41	-0.65	-2.76	No	Yes	No

Table S4: Continuation

Compound	Log S (mol/L)	Caco-2 Permeability (log Papp in 10^{-6} cm/S	Intestinal Absorption (%)	Fractional unbound (fu)	CNS permeability (logPS)	CYP3A4 inhibitor (Yes/No)	Hepatotoxicity	AMES toxicity
24	-4.61	**0.90**	86.82	0.06	-2.46	Yes	No	No
25	-4.87	0.66	76.65	0.12	-2.98	No	Yes	No
Verapamil	-5.23	1.11	97.10	0.009	-2.58	Yes	No	No

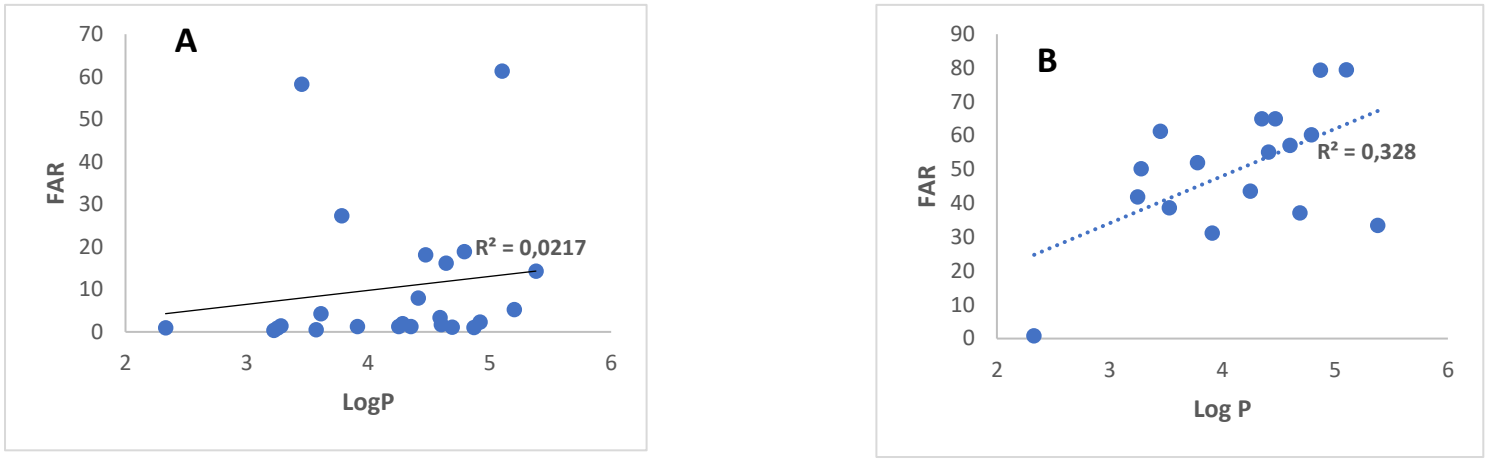

Figure S76: Representative plots of Log P versus FAR values for tested compounds in ABCB1-transfected mouse T-lymphoma cells at (A) 2 µM (compounds 1-25) and (B) 20 µM (compounds 1, 2, 4 and 12-25).

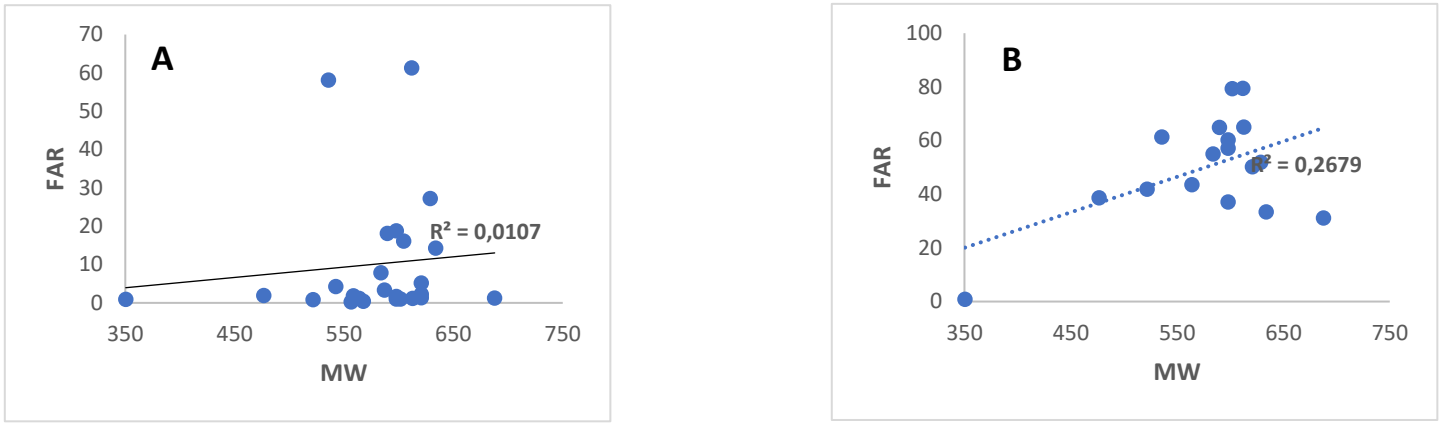

Figure S77: Representative plots of molecular weight (MW) versus FAR values for tested in ABCB1-transfected mouse T-lymphoma cells at at (A) 2 µM (compounds 1-25) and (B) 20 µM (compounds 1, 2, 4 and 12-25).

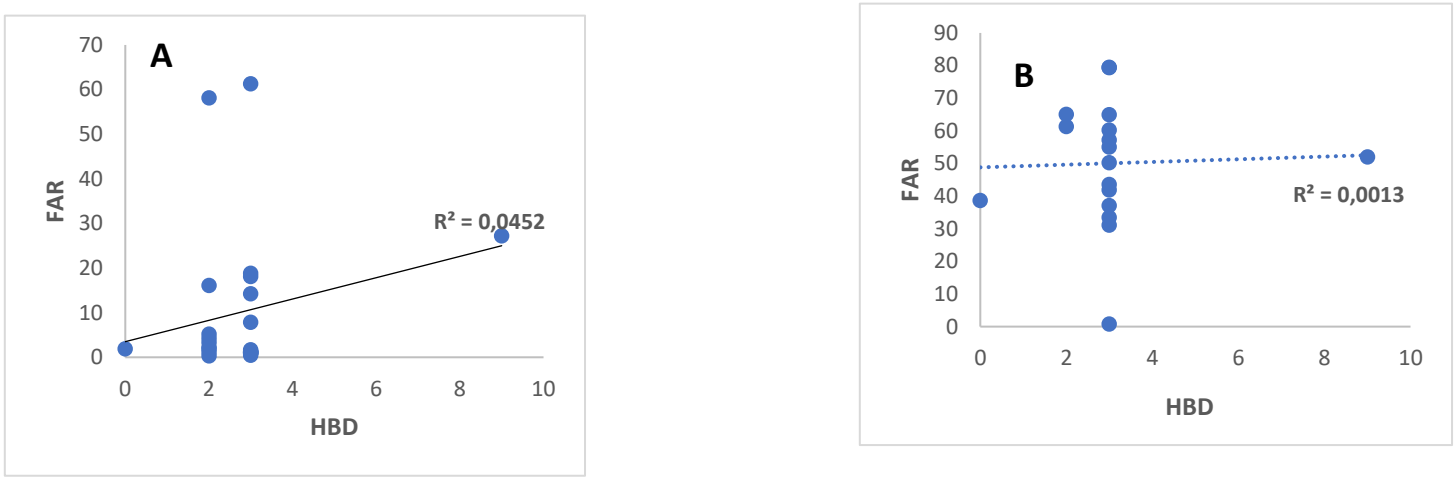

Figure S78: Representative plots of H-bond donors (HBD) versus FAR values for tested compounds in ABCB1-transfected mouse T-lymphoma cells at at (A) 2 µM (compounds 1-25) and (B) 20 µM (compounds 1, 2, 4 and 12-25).

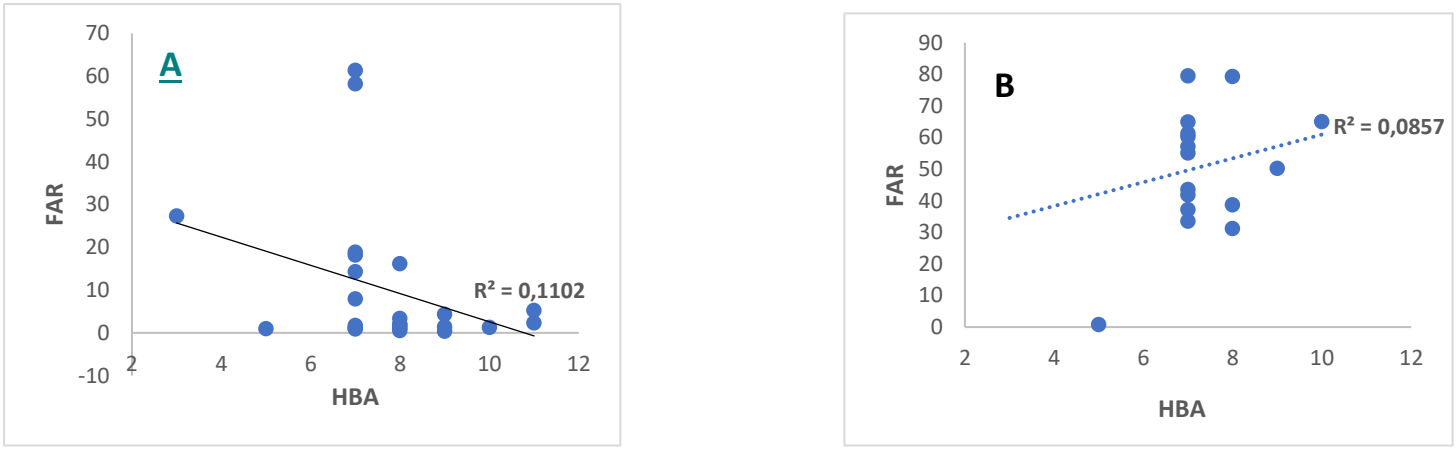

Figure S79: Representative plots of H-bond acceptors (HBA) versus FAR values tested compounds in ABCB1-transfected mouse T-lymphoma cells at at (A) 2 µM (compounds 1-25) and (B) 20 µM (compounds 1, 2, 4 and 12-25).

Figure S80: Representative plots of topological polar surface area (TPSA), versus FAR values tested compounds in ABCB1-transfected mouse T-lymphoma cells at at (A) 2 µM (compounds 1-25) and (B) 20 µM (compounds 1, 2, 4 and 12-25).

7. References

1 A. E. Owen, H. Louis, E. U. Ejiofor, W. Emori, T. E. Gber, I. Benjamin, C. R. Cheng, M. M. Orosun, L. Ling and A. S. Adeyinka, *Chem. Africa*, 2023, **6**, 2445–2461.

2 E. Villedieu-Percheron, V. Ferreira, J. F. Campos, E. Destandau, C. Pichon and S. Berteina-Raboin, *Foods*, 2019, **8**, 683–693.